Summer 2022

Effect of Metal-containing Nanoparticles on Bacterial Biofilms and on the Microbiome of Girardia tigrina

Azar Saikali
as915576@wcupa.edu

Effect of Metal-containing Nanoparticles on Bacterial Biofilms and on the Microbiome of *Girardia tigrina*

A Thesis

Presented to the Faculty of the

Department of Biology

West Chester University

West Chester, Pennsylvania

In Partial Fulfillment of the Requirements for the
Degree of
Master of Science

By

Azar Elie Saikali

August 2022

Acknowledgements

I would like to express my deepest appreciation to my advisor, Dr. John Pisciotta, for your patience, guidance, and support. Who has read my numerous revisions and helped make some sense of the confusion. I have benefited greatly from your wealth of knowledge and meticulous editing. Special thanks to my thesis committee members, Dr. Pagan and Dr. Chambers I appreciate your guidance and patience throughout this process. This project was made possible by a Cullen Grant to support student research and purchase supplies.

Finally, I must express my very profound gratitude to my parents and family for providing me with unfailing support and continuous encouragement throughout my years of study. This accomplishment would not have been possible without you. Thank you.

Abstract

Anthropogenically-produced nanoparticles are a form of nanotechnology being used in industries including food and textiles. Humans and livestock are frequently exposed to metal-containing nanoparticles (MCNPs), that have been washed into streams and rivers, have been deliberately used in food packaging as antimicrobials, preservatives or for supplementation. The animal microbiome, which consists of a diverse community of microorganisms, provides a number of benefits to the host in terms of nutrition availability, immune support, and can influence behavior. Biofilms of diverse microbes may cause detrimental effects, for instance by causing dental diseases in humans. However, the scientific community has not reached consensus on if direct contact with MCNPs is harmful to animals and or the microbiomes. This study exposed the microbiota of the planarian flatworm *Girardia tigrine* and developing microbial biofilms to MCNPs to investigate their effect on biofilms and the microbiome of this model organism. Zinc oxide (ZnO), copper silicon (CuSi), and tribasic copper chloride (TBCC) nanoparticles were used at 6 different concentrations. ZnO NPs, CuSi NPs, and TBCC NPs, inhibited the formation of a mixed community plastic-adherent biofilm as determined by plate assay. The pure culture *Staphylococcus aureus* F-182 biofilm was inhibited by ZnO NPs and CuSi NPs but was not inhibited when exposed to TBCC NPs. The planarian microbiome experienced a pronounced shift from Betaproteobacteria to Gammaproteobacteria when exposed to ZnO NPs, and CuSi NPs. Of the MCNPs CuSi NPs increased the diversity of the microbiome while TBCC treatment induced minimal microbiome disruption as compared to untreated control.

Table of Contents

List of Tables

List of Figures

Introduction

Gut Microbiome

The microbiome is a complex community of microorganisms consisting of bacteria, viruses, protozoa, and fungi, living in different districts of the human body, such as the gastroenteric tube, skin, mouth, and respiratory system (Sender *et al.*, 2016). Over 70% of the human microbiota lives in the gastrointestinal tract, steadily increasing in species diversity from the gastric lumen to the large intestine (Pascale *et al.*, 2018). The microbiome of the GI tract has co-evolved with the host to form an intricate mutualistic symbiotic relationship. The development of the human gut microbiome begins immediately after birth and its composition is strongly influenced by the type of birth, whether natural or cesarean, the individual's genetics, and environmental factors (Backhed, 2015). The gut microbiota is heavily influenced by host nutrition whether it be artificial, heavily processed, or natural products (Pascale *et al.*, 2018). The microbiome provides the host with help in maintaining the integrity of the mucosal barrier, providing nutrients such as vitamins including short-chain fatty acids, B vitamins, and vitamin K, protecting against pathogens, and regulating host immunity (Thursby & Juge, 2017).

Bacteria of the gut microbiome can promote cell renewal and wound healing in the case of *Lactobacilli rhamnosus* (Swanson II *et al.*, 2011). Several other species have also been implicated in promoting the epithelial integrity and bacteria modulate mucosal properties and turnover (Thursby & Juge, 2017). Petersson investigated the role of the mucus barrier in induction of colitis in mice (Petersson, 2011). Mice raised in a germ-free environment had an extremely thin adherent colonic mucus layer, which can result in colonic bacteria invading the mucosa and causing inflammation. Bacterial products such as peptidoglycan and lipopolysaccharides were found to increase the thickness of the adherent mucus layer and was

restored to levels that were observed in conventionally reared mice (Petersson, 2011). Germ-free mice have reduced expansion of CD4+ T-cell populations which is a major immune deficiency. However, the deficiency was reversed by the treatment of germ-free mice with polysaccharide A from the capsule of *Bacteroides fragilis* (Mazmanian, 2005). Such microbial effectors mediate processes that can ameliorate certain inflammatory gut disorders and help differentiate between beneficial and pathogenic bacteria and increase the number of immune cells (Hevia, 2015). *B. fragilis* can also secrete membrane vesicles that reduce gut mucosal inflammation via regulatory T cell-independent mechanisms (Chu 2016).

The gut microbiome facilitates strengthening of the epithelial wall and mucosal membrane, of the gut, as well as providing nutrition. The major fermentation products in healthy adults are gases and organic acids, particularly the three short-chain fatty acids (SCFAs) acetate, propionate, and butyrate (Louis, 2014). The three SCFAs are typically found in a 3:1:1 ratio, and they play a key role in the maintenance of gut and metabolic health (Louis, 2014; Blaak, 2020). These SCFAs are absorbed by the epithelial cells of the GI tract that are involved in maintaining the mucosal barrier and they use the SCFAs in the regulation of cellular processes such as gene expression, chemotaxis, differentiation, proliferation, and apoptosis (Corres-Oliveira, 2016). Acetate is produced by most gut anaerobes whereas propionate and butyrate are produced by different subsets of gut bacteria such as *Faecalibacterium prausnitzii* and *Eubacterium rectale* (Louis, 2017). Butyrate is formed from acetyl-CoA whereas propionate, depending on the nature of the sugar, has two pathways: the succinate or the propanediol pathway (Louis, 2017). Butyrate is known for its anti-inflammatory and anticancer properties; it can also attenuate bacterial translocation and enhance gut barrier function by affecting tight-junction assembly and mucin synthesis (Morrison, 2016). There are many other gut microbial products helpful to the survival

of the host. For example, lactic acid bacteria are probiotic microorganisms commonly found in yogurt that are involved in the production of vitamin B12, which cannot be synthesized by either animals, plants, or fungi. *Bifidobacteria* are main producers of folate, a vitamin involved in vital host metabolic processes including DNA synthesis and repair (Thursby& Juge, 2017). Colonic bacteria can also metabolize bile acids that are not reabsorbed for biotransformation to secondary bile acids. The human gut microbiota has also been shown to synthesize vitamin K, riboflavin, biotin, nicotinic acid, pantothenic acid, pyridoxine, and thiamine (Leblanc, 2013).

One of the roles of the animal microbiome is to defend the host against pathogens. Modification in the microbiota composition can lead to several diseases, including metabolic diseases, such as obesity, diabetes, and cardiovascular disorders (Pascale, 2018). Some properties of the microbiota have been researched and understood, such as digesting foods and assisting the immune system in defending against pathogens. Recent research indicates the microbiome, shaped largely by diet, plays a role in the behavior and regeneration of an organism. The use of nanoparticles has expanded into various industries including food manufacturing, which has allowed metal containing nanoparticles (MCNPs) to access the human gastrointestinal tract (Ghebretatios *et al.,* 2021). Little is known about how they may impact human health and as the gut microbiome continues to be increasingly implicated in various diseases of unknown etiology, researchers have begun studying the potentially toxic effects of these MCNPs on the gut microbiome (Ghebretatios *et al.*, 2021). The microbial flora live in communities forming biofilms that reside in the saliva, gastrointestinal tract, oral cavity, ear canal, and mucosa and help mammals in numerous metabolic activities, including ATP production, vitamin synthesis, and in the innate defense mechanisms against pathogens (Rimondini *et al.*, 2014) In some instances, however, the growth of these mutually beneficial microorganisms can become

uncontrolled, leading to infection (Bjarnsholt, 2013; Rimondini *et al.*, 2014). Bacterial infections are the most common type of acute and chronic infections causing worldwide morbidity (Khatoon *et al.*, 2018).

Planaria

Planarians are a series of several species of free-living flatworms that display bilateral symmetry (Pagan, 2017). Planarians have long been known to possess astonishing regenerative capabilities. If a planarian worm is chopped into three pieces, each of the piece's regenerates back into a complete and perfectly proportioned animal within 2 weeks (Ivankovic, 2019). Hundreds of planarian species exist worldwide in marine, freshwater or terrestrial habitats and the regenerative abilities vary greatly among different species (Ivankovic, 2019). Freshwater planaria have been used as testing models in various scientific fields, such as aging, pharmacology, drug abuse, human diseases, ciliary assembly and motility, chemical toxicity, teratogenicity, tumorigenicity, neurotoxicology, carcinogenicity, stem cell biology and regenerative medicine (Wu and Li, 2018).

Since the 1970's, planarians have been understood to be model organisms in pharmacological studies related to drug abuse for several reasons. Planarian possesses a primitive brain that has many features in common with vertebrate nervous systems, such as multipolar neurons and dendritic spines, they also possess nearly every neurotransmitter that has been found in mammals (Pagan *et al.*, 2012). Planaria, due to their shared neurotransmitters, display behaviors associated with drug abuse; specifically withdraw-like behaviors similar to humans. Consequently, planarian are ideal organisms to study drug abuse and neurological diseases (Pagan, 2017).

Planaria are extremely sensitive to low concentrations of harmful substances in aquatic ecosystems and are widely used as water quality indicator species to provide early warning of harmful pollution in aquatic ecosystems (Ding *et al.,* 2019; Hagstrom *et al.,* 2017). Some rivers of Malaysia have been examined for AgNPs and have found concentration of 10 μg/ml (Syafiuddin, 2018; Bijnens *et al.*, 2021). When the planaria *Schmidtea mediterranea* was exposed to AgNPs in a heterogenous mixture, at the same levels found in Malaysian rivers, it displayed sublethal adverse effects (Leynen, 2019).

At lower NP concentrations planaria may not display behaviors associated with toxic substances but may have induced changes within their microbiome. Bijnens *et al*., 2021 observed a shift of the microbial composition of the microbiome of *S. mediterranea*. The impact of these bacterial community shifts on planarian health and physiology is still unknown and need to be investigated to fully assess toxicity of NPs (Bijnens *et al.*, 2021). The exact role of the microbiome in the planaria remains to be fully elucidated; however, it is known that a pathogenic shift in the microbiome of planaria impedes tissue regeneration (Arnold et al., 2016).

Planarian Microbiome

Few studies have analyzed the microbiome of planaria species and even fewer have researched the effects of NPs on the microbiome of planaria. Of these, one exposed the microbiome of the planarian *Dugesia japonica* to microplastics and measured the effects through 16S rRNA gene sequencing, a form of metagenomic analysis. In unexposed microbiomes, Proteobacteria were found to be dominant in *D. japonica* microbiome with some of the genera detected identified as *Rhodoferax, Chryseobacterium*, *Pseudomonas*, and *Enterobacter* (Han *et al.*, 2022).

To determine the toxicity of Ag NPs, *Schmidtea mediterranea* was used as the model organisms. The relative composition of bacteria in non-exposed *S. mediterranea* mainly consisted of representatives of the phyla Proteobacteria and Bacteroidetes, with the dominant classes being Gammaproteobacteria and Bacteroidia (Bijnens *et al.*, 2021). Proteobacteria comprised of the order Betaproteobacteriales, family Burkholderiaceae, and the genera *Curvibacter* and *Undibacterium.* The phyla Acidobacteria, Actinobacteria, Armantimonadetes, Firmicutes and Planctomycetes were also present, although their relative abundance was less than 1% averaged over worm samples not exposed to Ag NPs (Bijnens *et al.*, 2021). The planarian *Stenostomum leucops* was used in a study about the microbiome's role in host gene expression. A comparison of the microbiomes found in the three strains of Stenostomum analyzed showed that it was highly variable in the number and composition of microbial species. Of a total of 156 species, only one bacterial taxon (*Bacillus cereus* sp. group) was shared by all strains (Rosa and Loreto, 2019).

Bacterial Biofilms

Biofilms are found in almost every aspect of our lives and play a significant role in the survival of many organisms on this planet. However, there are also negative consequences of biofilms which include their defining role in an extensive variety of infections (Costerton *et al.*, 1999) and their role in the biofouling of surfaces which has negative impacts in the process industries (Fulaz *et al.*, 2019). A biofilm is an organized aggregate of microorganisms living within a self-produced matrix of extracellular polymeric substances (EPS) that is attached to a surface (Yin *et al.*, 2019). Biofilms can form on virtually any surface providing all the necessary components for the biofilm's survival are present. Biofilms form on teeth, as dental plaque, in our guts as the microbiome, rocks as photosynthetic algae, in pipes, and even on medical

implants. Biofilm formation begins when a planktonic bacterium meets a surface that best describes its niche. That individual bacteria will form pili and fimbria to bind to the surface temporarily and then permanently. After a couple of hours or days, depending on the species of bacteria, other bacteria and microbes will be recruited and become part of the biofilm, this would form a microcolony. The aggregate of bacteria will start to produce a sticky/slimy matrix that consists of extracellular polymeric substances (EPS). EPS are mainly composed of polysaccharides, proteins, lipids, and nucleic acids, which form a highly hydrated polar mixture that contributes to the overall scaffold and three-dimensional structure of a biofilm (Yin *et al.*, 2019).

Cells within biofilms are resistant to many different environmental insults, including UV damage, metal toxicity, anaerobic conditions, acid exposure, salinity, pH gradients, desiccation, bacteriophages, and amoebae (Hall-Stoodley *et al.*, 2004; Costerton *et al.*, 1999; Römling & Balsalobre, 2012). Biofilms also can defend against a range of chemically diverse biocides and antibiotics that are utilized in industrial and clinical settings. Biofilms that develop on medical implants impose a dangerous and persisting problem for the patients. Biofilms that have formed on implanted medical devices cause chronic infections which can only be treated by their removal and leads to the un-affordable treatment as well as mental illness to patients (Costerton *et al.*, 2005; Høiby *et al.*, 2011). Biofilms have at least three proposed mechanisms of resistance that include, reduced penetration of antimicrobials into the biofilm, inactivation of antimicrobial agents by EPS components and, the altered metabolic state of bacterial cells within the biofilm (Flemming *et al.*, 2016; Bertoglio *et al.*, 2018).

The biofilm matrix serves as a physical barrier and their thickness and chemical composition can prevent the perfusion of antimicrobials such as antibiotics (Dunne, 1993). A

small portion of the antibiotics are able to pass through the barrier but are faced with the polar EPS molecules that bind to charged antibiotics and form a shelter for microorganisms (Nadell, 2015). This allows the microbes associated inside the biofilm to establish a tolerance to the antibiotics (Fuente-Nu´n˜ez, 2013), increasing the number of antibiotic-resistant bacteria strains, which results in the prevalence of untreatable bacterial infections. EPS causes the formation of different gradients inside the biofilm community such as nutrient, oxygen and, pH (Flemming, 2016; Flemming *et al.*, 2016) and this leads bacteria to respond differently based on the condition they find (Bertoglio *et al.*, 2018). Low nutrients and oxygen paucity may lead to a dormant state, in which these so-called persister cells are still viable but not actively proliferating, being therefore non-susceptible to most antimicrobial treatments (Brown *et al.*, 1988; Lewis, 2007). Efflux pumps such as the PA1874-1877 in *Pseudomonas aeruginosa*, is used to transport antibiotics to prevent toxic accumulation (Zhang & Mah, 2008). These efflux pumps are expressed more in the biofilm state compared to the planktonic state (Poole, 2001) attributing to the biofilm's resiliency. Novel methods and materials are needed to disrupt harmful microbial biofilm communities that develop around one or more keystone species. For instance, *Streptococcus mutans* is a facultatively anaerobic, sucrose fermenting bacterium important for dental plaque formation and cavity formation.

Nanoparticles

Nanoparticles (NPs) encompasses a small niche in the world of nanomaterials. Nanoparticles measure from 1 – 100 nm in at least one dimension. Many exist naturally, some are synthesized by organisms, are created as a by-product of human activity, and are purposely produced to perform specialized functions. MCNPs can be classified as either organic, when made from molecules like dendrimers, liposomes, and polymeric nanoparticles, or can be

classified as inorganic, when comprised of fullerenes, quantum dots, and gold. MCNPs can be given types of protective coatings that provide some beneficial function, such as to prevent agglomeration of particles in suspension or a synthetic polymer that acts as a stabilizing agent for metal MCNPs (Leyen, 2019). As an example, silver MCNPs (Ag NPs) are coated in polyvinylpyrrolidone (PVP), a synthetic polymer that chemically stabilizes the NP against oxidation (Liu, 2013; Desireddy, 2013). Form and function of nanoparticles are dictated by the material for which it is composed of. Liposomes are lipid-based vesicles that are extensively explores and the most developed nanocarriers for novel and targeted drug delivery (Bhatia *et al*, 2016). Liposomes, depending on their size and number of bilayers, can be classified into three basic types: Multilamellar, Small unilamellar, and Large unilamellar vesicles. Furthermore, liposomes are prepared with distinct structure, composition, size, and flexibility with variety of surface modifications, making the most intelligent carrier system for both active and passive delivery of bioactive (Bhatia *et al*, 2016). Carbon based nanomaterials (CBNs) are simply carbon atoms bonded in varies ways to create distinct shapes. CBNs exert an effective biocidal action against a broad spectrum of bacteria, viruses, and fungi, including multidrug-resistant strains (Salesa *et al.*, 2019; Innocenzi *et al.*, 2020; Wang *et al.*, 2014). CBNs have shown potent antiviral activity against a broad range of enveloped positive-sense single-stranded RNA viruses, including SARS-CoV-2 (Łoczechin *et al.*, 2019). The development of CBNs as antiviral agents is possible because they possess a high surface area that allows their functionalization which further enhances their biocompatibility and therapeutic efficacy (Serrano-Aroca *et al.*, 2021). Because of the widespread use of anthropogenic nanoparticles, it is inevitable that some of these manufactured MCNPs will leak into the environment, for example in waste streams. It is

important to understand nanoparticles in waste and in the environment and to understand the effects that they may have on animals and microbes.

Antimicrobial Properties of MCNPs

Depending on the composition of the nanoparticles it can possess properties that may cause lethal effects in microbes. In the case of MCNPs their most prominent feature is their ability to release metal ions when exposed to air, water, or saline solutions. The metal ions released from MCNPs were found to interact with the thiol (-SH) groups, in proteins and enzymes, reducing them to metal atoms the interaction of metal ions and thiol groups inactivates the essential metabolic proteins for respiration (Raghunath & Perumal, 2017). Metal ions will also interact with the thiol groups in the peptidoglycan layer, disrupting the cell wall making it permeable to MCNPs (Raghunath & Perumal, 2017). Once in the cells the MCNP can induce the generation of reactive oxygen species (ROS) triggering oxidative stress.

MCNPs induce oxidative stress in both eukaryotic cells and bacterial cells. Oxidative stress is a state of redox disequilibrium, which occurs when ROS production exceeds the antioxidant defense capacity of a cell (Deres *et al.*, 2005). Normally ROS, which include superoxide anion, hydrogen peroxide and the hydroxyl radicals are used for cell signaling are tightly regulated by the cell to prevent internal cellular damage. MCNPs induce the generation of ROS by interacting with molecular oxygen on reactive sites on the surface of the NP. Elevated levels of ROS are associated with molecular damage to cellular components and, consequently, tissue injury in animals (Swanson, 2011).

Enzymatic disruption can be caused by nanoparticles. Respiratory enzymes including succinate dehydrogenase and ATP synthase are damaged by ROS generated from MeO-NPs, which eventually results in cell death (Raghunath & Perumal, 2017). This oxidative stress has

been observed in many metal-containing NPs. In the case of AgNPs, silver acts as a weak acid and has the tendency to react with bases such as sulfur and phosphorus, which are main constitutes of protein and DNA. This results in AgNPs causing damage to DNA and inactivating proteins which will lead to the cells death (Raghunath & Perumal, 2017). Cytochrome P450 (CYP450) is an enzyme that is found abundantly in the brain and liver, it metabolizes exogenous and endogenous compounds, such as antidepressants, opiates, steroids, arachidonic acid, dopamine, and serotonin (Wang, 2019). It is understood that CYP450 expression can be regulated by oxidative stress via the activation of nuclear transport (Tolson, 2010). Copper NPs (Cu NPs) increase ROS generation and decrease antioxidant enzyme activity (Zhang, 2015). When rats were exposed to Cu NPs for 28 days their brain CYP450 protein expression levels decreased (Wang, 2019). The associated changes of CYP450 may be important for the development of drugs that act and are metabolized locally in the brain, as well as therapeutics that directly target brain CYPs (Navarro-Mabarak *et al.*, 2018).

Not all metal containing MCNPs are toxic. In the food industry TiO_2 (E171) has been applied as an additive to enhance the white color of certain products, such as sweets or milk-based products (Musial, 2020). TiO_2 NPs unlike other MeO NPs does not generate ROS in bacterial or animal cells, instead they react with cellular structures that are involved in the process of respiration and block ROS formation (Musial, 2020). To simulate long-term, low dose ingestion of E171 in humans, TiO_2MCNPswere injected in Wistar rats for 60 days and were found to possess genotoxic effects (Grissa, 2015). Intragastric E171 exposure was observed increasing tumor progression markers and enhanced tumor formation in the distant colon in a murine model (Urrutia-Ortega, 2016). Although it should be noted that TiO_2MCNPsdid not

induce tumor formation itself but led to dysplastic changes in colonic epithelium and a decrease in goblet cells (Musial, 2020).

The morphology of MCNPs can have an effect on how well the NP performs as an antimicrobial agent. Ag NPs between the ranges of 1 – 10 nm were observed to attach to the surface of a cell membrane and drastically disturb its proper function (Morones, 2005). Nanoparticles can cause toxicity to microbes by physically damaging membranes and cell walls. Ag NPs with diameters of 10nm, 75nm, and 110nm were studied for their bacterial toxicity. The Ag NP with a diameter of 10nm had the greatest bacterial toxicity on microbial populations in the ileum and the most pronounced impact on host gene expression (Williams, 2014). A similar study collected data from mammalian ileal tissues that were exposed to Ag NPs and found that NP size and bactericidal activity were negatively correlated (Williams, 2014). Depending on the method used to create MCNPs the morphologies displayed could be from a selection of varieties including nanocubes, nanoprisms, nanospheres, triangular nanoplates, and rod-like shapes. MCNPs bacterial toxicity can vary depending on the morphologies the MCNPs take up. Triangular Ag nanoprisms exerted greater bacterial toxicity due to the sharp edges of the triangular shape. Truncated triangular Ag NPs displayed stronger biocidal action than spherical and rod-shaped NPs. The morphology of Ag NPs affects antibacterial activity in terms of specific surface areas and facet reactivity and those with larger effective contact areas and higher reactive facets exhibit stronger antibacterial activity (Li, 2018).

Nanoparticles and The Microbiome

Some nanoparticles, such as ZnO, possess properties that are effective against microbes which makes them useful as preservatives in the food and medical industries. The whitening imparted by ZnO is further utilized as a processed food coloring agent, for example in frostings.

The unregulated use of MCNPs in these industries could allow MCNPs to be leaked into the environment and pose a potential threat to humans, animals, plants, insects, and microbes. Certain MCNPs pose a threat to living organisms and can disrupt the gut microbiome and the intestinal epithelial barrier of living organisms (Li, 2018). A disruption of the gut microbiome, also known as dysbiosis, which is linked to medical conditions including, colitis, inflammatory bowel disease, diabetes, and metabolic syndrome (Williams, 2014). Better understanding of NPs, in particular metal-containing nanoparticles, on the microbiota will provide us with the knowledge necessary to avoid the negative adverse effects that MCNPs may possess.

Copper oxide nanoparticles (CuO NPs) were found to disrupt the microbiome of collembolans, which are primitive hexapods known as spring tails. The Cu exposure has a profound influence on the gut microbiota of collembolans both decreasing their microbial diversity and shifting their microbial community structure (Ding, 2020). Hens exposed to Zinc Oxide NPs (ZnO NPs) and had their ileal microbiota sequenced and the bacterial community richness of the ileum was reduced as the dosage of MCNPs increased (Feng, 2017). *Lactobacillus* is the predominant bacterium in animal and human ileum, and it was observed that it had a negative correlation with ZnO NP exposure. This change to the composition in the avian intestinal microbiota can be problematic (Ghebretatios, 2021). Distinct species may react differently to nanoparticles.

In some circumstances MCNPs may be beneficial in terms of their effect on the microbiota. A study administered AgNPs in the drinking water of experimental mouse models with ulcerative disease and Crohns disease. Interestingly, the AgNPs effectively alleviated the colitis of the mice (Li, 2018). ZnO NPs have similarly been indicated to have positive impacts on the gut microbiota of some host animals. The bacterial richness and diversity of the microbiota in

the ileum of piglets were increased when exposed to ZnO NPs (Xia, 2017). In contrast to the case with chickens, when administered to piglets, ZnO nanoparticles have a growth promoting effect (Pei, 2018). Copper containing nanoparticles, such as tribasic copper chloride (TBCC), are commonly used for growth promotion in animal farming and can bolster aspartate transaminase (AST) and the levels of antioxidant enzymes such as super oxide dismutase (SOD) (Zheng, 2017). In humans and other animals, MCNPs could play a key role in the future treatment of GI diseases. However, many of the mechanisms, particularly those related to perturbation of host microbiome, are unknown and research is needed to comparatively assess the effect of disparate MCNPs on model organisms (Ding, 2020; Ghebretatios, 2021).

Nanoparticles and Biofilms

Biofilms are dynamic entities, with their structure and material/chemical properties continuously mediated by biochemical and physicochemical factors which are, in turn, influenced by the local environmental conditions (Petosa *et al.,* 2010). This interplay adds to the complexity of NP transport into biofilms (Fulaz *et al.,* 2019). Interactions between MCNPs and biofilms can be described by three sequential mechanisms (Ikuma *et al.,* 2015): transport of MCNPs to the biofilm–fluid interface; attachment to the biofilm surface (outer region); and migration within the biofilm. At each of these steps, the interactions are a complex interplay of factors such as, EPS matrix viscosity, cell density, liquid flow, external mass transfer resistance, physicochemical interactions of the MCNPs with EPS components, and the characteristics of the water spaces (pores) within the EPS matrix (Miller *et al*., 2015). On first coming into contact with a biofilm, MCNPs interact with a complex mixture of macromolecules that alters their surface properties, and the different properties are ascribed to the so-called ’biomolecular corona’ (Mu *et al.,* 2014; Ke *et al.,* 2017), often referred to as a ’protein corona’ (Doctor *et al.,*

2015). The nature of this corona influences the NP–biofilm interactions (Ikuma *et al.*, 2015) by altering the physicochemical characteristics of MCNPs such as the size, shape, surface charge, hydrophobicity, and functional groups. In depth research has yet to be done on the interactions of MCNPs and biofilms. Studies need to be conducted on the properties of the protein corona and their effect on the nanoparticle's antimicrobial ability.

Accordingly, the goal of this study was to determine the efficacy of MCNP on the destruction of biofilms. It was hypothesized that: MCNPs are able to inhibit biofilm formation of a pure cultured biofilm and a mixed community biofilm culture. The study also focuses of the effect than MCNPs may possess when introduced to the microbiome of *Girardia tigrina*. It was hypothesized that MCNPs are able to change the microbial composition of the gut microbiota of *Girardia tigrina*.

Materials and Methods

Preparation of Nanoparticles

In this study the process of metal electrolysis was used to create the MCNPs. Metal electrolysis involves a metal anode, such as zinc, whose electrons are to be sacrificed to a metal cathode, such as copper. The transfer of electrons oxidizes the anode thus creating metal nanoparticles, in this case Zinc Oxide NPs (figure 1). It is a facile and cost-effective technique for the production of nanoparticles which are insoluble in aqueous or non-aqueous electrolytes (Pourmortazavi *et al.,* 2015).

Tribasic Copper Chloride (Cu_3Cl), Silicon (Si), Zinc Oxide (ZnO), and Silicon Copper (SiCu) nanoparticles were used for this study and were synthesized by Kolasinski Labs and the Pisciotta Lab at WCU. For the creation of ZnO and TBCC NPs, 100ml of 100nM NaCl solution was added to a 110 ml serum bottle with a rubber stopper. The copper cathode, ~5cm in length, and the appropriate anode, ~7.5 cm in length, (Iron for TBCC and Zinc for ZnO) was pushed into the stopper until about 0.5 - 1 cm of the wires were exposed on the top and without the wires touching. A needle was placed through the stopper to allow the hydrogen gas to escape. An Arksen DC Power Supply 303D was set to 10V and was allowed to run for 1 hour under a flow hood, to properly dispose of the H_2 gas (Figure A). The NPs, depending on the type of metal, may interfere and decrease the current of electricity from the power supply. Periodically, during the process gently swirl the bottle to allow the MCNPs to detach from the anode to prevent any interactions between cathode and anode. After the process, the serum bottle was then tilted on an angle for 72 hours to allow the MCNPs to settle (Figure B). After the MCNPs settle to the bottom of the serum bottle half of the salt solution was removed, without disturbing the NPs. A vacuum flask and a filter funnel with a filter paper was used to separate the MCNPs from the

suspension. A sterile serological pipette was used to transfer the NP suspension to the filter paper (Figure C). The MCNPs suspension was slowly dripped onto the filter paper to cover it entirely without going over the edges. The filter paper with the MCNPs (figure D) was then placed in empty petri-dishes and set in a 55°C incubator to dry. The dry MCNPs were collected into a 1.5 ml Eppendorf tube.

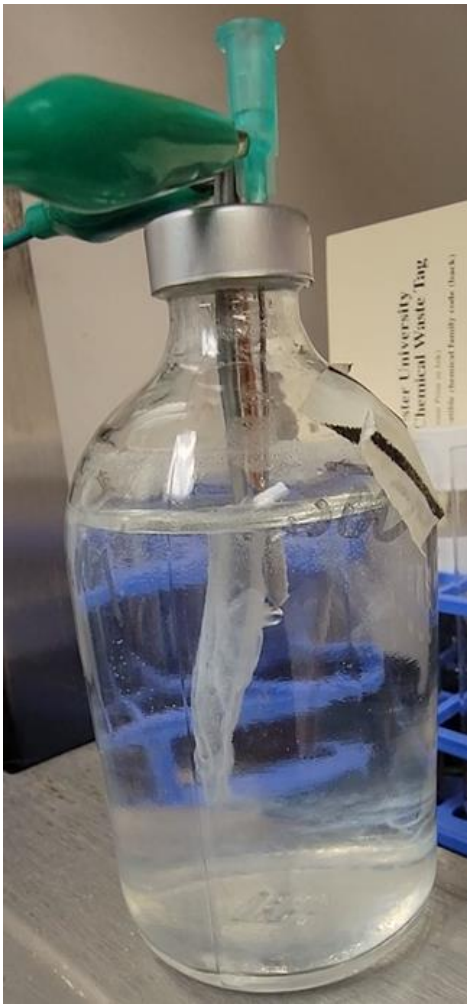

Figure 1) ZnO NPs beginning to form on the Zn anode.

Figure 2) Serum bottle laid on test tube rack to allow ZnO NPs to precipitate for easier extraction.

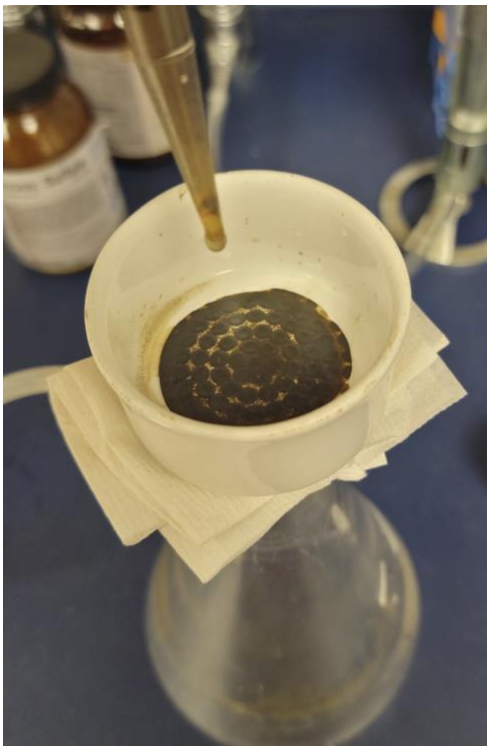

Figure 3) Filtering out TBCC NPs from the suspension. Cloth between the funnel and flask to create better suction.

Figure 4) Dried ZnO NPs on quantitative filter paper.

Mix Biofilm Sampling

Sterile **c**otton swabs were used to sample areas suspected of having biofilm growth. After swabbing the sampled were placed in 15 ml Falcon tubes containing lysogeny broth. Three areas were suspected of having biofilm growth; the office aquarium in the biology department at West Chester University of Pennsylvania (WCUPA), A mix of three protist jars from Columbia (*Arcella vulgaris, Paramecium bursaria,* and *Euplotes*), and the inside of a hose used to dispense DI H_2O in Merion Lab 312 at WCUPA.

Two plates were created, one was incubated at 31°C with shaking at 200 rpm while the other plate was incubated at 31°C without being shaken. Both plates were incubated for 48 hours. Each sample had 9 wells (3x3) each with 200µl of sample to have three replicates each in triplicate. After incubation, the absorbance of the plates was measured at 595 nm using the Synergy™ 2 Multi-Detection Microplate Reader by BioTek Instruments, Inc.

Development of the Selected Biofilm

During previous biofilm and NP assays biofilms would tend to be distorted and washed away during the rinse process of the crystal violet staining procedure. To prevent this from happening in future experiments, a plastic-adherent biofilm was developed. Developing a plastic adherent biofilm required the selection of the biofilm formers to ensure all microbes of the mix culture participated in the structural integrity of the biofilm

Two hundred microliters of the original mixed biofilm suspension were aliquoted into a well of a 96 MWP and was incubated for 5 days at room temperature in the dark. After incubation the supernatant was removed, the biofilm was resuspended in 200 µl of LB and was aliquoted into a new sterile well in the MWP. The second biofilm sample was incubated for 3 days at room temperature in the dark. This was repeated for a total of 5 wells with 3-day incubation at room temperature in the dark. After the fifth well was incubated the resuspended biofilm was transferred into a 15 ml falcon tube containing LB. The resulting biofilm should be selected for plastic adherence.

Preparation of Biofilm Culture for Nanoparticle Testing

The bacteria used to form the biofilm (biofilm formers) were allowed to enter Log phase of growth by incubating the suspension at 37°C for 2 hours. The biofilm suspension consisted of 20 ml of Lysogeny Broth (LB) in a 50 ml Falcon tube with 10 µl of the bacterial biofilm suspension. After incubation, the absorbance was measured on the spectrophotometer at 600 nm. The suspension was diluted with LB until an OD of 0.05 was reached which equates to roughly 5.0×10^7 CFU/ml.

Dilution of Metal Containing Nanoparticles

Three separate series of experiments—with identical experimental setups—were run in triplicate to assess the effect of ZnO, CuSi, and TBCC NPs in 200 µl samples. Stock NP suspensions of 1 mg/ml and 2 mg/ml were created by weighing out MCNPs and mixing with deionized water in 1.5ml Eppendorf tubes. The studied NP suspensions at different concentrations were aimed at 0.01, 0.10, 0.15, 0.25, 0.50, 1.00 mg/ml final NP nominal concentration in each well. The experimental NP suspensions were diluted with Lysogeny broth (LB). The proportion of LB in the negative and positive control was the same as in the NPs-containing samples

Biofilm Nanoparticle Treatment

A flat bottomed, clear, 96 multi-well plate (MWP) was used to grow and measure the biofilm growth of *Staphylococcus aureus* F-182 and the glass-adherent aquarium-derived biofilm. The first two rows were reserved for the positive and negative control. The other six wells are used for the experimental samples. 100 µl of NP concentration was aliquoted to each well starting with the lowest concentration. 100 µl of biofilm suspension was then added to each experimental well and to the positive control well. 200 µl of LB was added to the negative control well and 100 µl was added to the positive control well. Each well of the MWP had a final volume of 200 µl.

The Synergy 2 spectrophotometer was used to measure the absorbance and represent growth of biofilm. An initial time point 0 absorbance was measured at 595 nm. The mixed community biofilm samples were incubated at room temperature for 24 hours in the absence of light. The *S. aureus* biofilm samples were incubated at room temperature for 48 hours in the absence of light. An absorbance reading was taken after incubation of the MWP at 595 nm. The

samples of the MWP were then stained and had the absorbance measured to quantify biofilm growth.

	Sample 1				Sample 2				Sample 3			
	1	2	3	4	5	6	7	8	9	10	11	12
+												
-												
0.01 mg/ml												
0.10 mg/ml												
0.15 mg/ml												
0.25 mg/ml												
0.50 mg/ml												
1.00 mg/ml												

Table 1. Lay out of MWP for biofilm assay. First row was reserved for positive control and the second row was reserved for the negative control. Remaining rows contained NPs, increasing in concentrations in descending order. Each sample was tested in 3 replicates as indicated by the highlighted columns.

Biofilm Staining

To better visualize the biofilm in the spectrophotometer 200µl of crystal violet stain (CV) was added to the positive control, negative control, and experimental wells. CV was left in the wells for a at least 5 minutes to ensure the biofilm was fully saturated with CV. After the 5 min the CV dye was disposed of and the MWP was submerged in water to remove the CV that has

not bound to the biofilm. The MWP was submerged three separate times, each time with fresh water in order to remove as much excess dye as possible. In order to dry the MWP it was blotted dry on paper towels until all excess liquid was removed. If blotted to aggressively there is a possibility for the biofilms to detach and obscure results. To quantify the stained biofilm the 96-microplate spectrophotometer was set to 595nm and the absorbance of the MWP was measured.

Planaria Nanoparticle Assay

Girardia tigrina planaria of similar age and size (approximately 4 – 6 nm) were purchased from Carolina Scientific and cultivated in artificial pond water at room temperature. The planaria were kept at room temperature (24°C) and in the absence of light. One planarian was used for each replicate for experimental sets and controls. For each nanoparticle type tested, there were to be three replicates for each concentration. A negative control set devoid of MCNPs was included to examine the natural microbiome. Before exposure to MCNPs the planarians were starved for seven days before exposing them to nanoparticles, this is to prevent DNA from the food from interfering with the microbial DNA (Leynen, 2019).

For exposure with nanoparticles, each experimental planarian set was be placed in 10 ml of artificial pond water (APW, NaCl, 6 mM; $NaHCO_3$, 0.1 mM; $CaCl_2$, 0.6 mM) in sterile plastic Petri plates containing the desired nanoparticle concentration (1-10 mg/ml). The plates were kept in a dark place at room temperature for 7 days. Planarian worms were monitored each day of the testing period. Planarian survival, motility and behavior was observed and recorded for toxicity and adverse effects of the MCNPs. Worms were exposed to 10 ml of unadulterated APW for the untreated control.

Biolog EcoPlate™

The Biolog EcoPlate™ is a low-cost, convenient, and rapid technique for investigating the physiological diversity in the environment and provides information about community-level physiological profiles (CLPP) (Nemeth *et al.*, 2021). The EcoPlate™ contains 96-wells that contain pre-dried carbon sources and a tetrazolium violet redox dye that turns purple if the added microorganisms utilize the carbon source (Bochner, 1989). The study investigated the time-dependent effect of MCNPs on the biodiversity and functionality of the microbiota of *Girardia tigrina*.

Planarian samples were exposed to 0.1 mg/ml of MCNPs suspension for 1 week before transfer to Biolog EcoPlate™. After exposure the planarians were washed of any NP residue in Sterile DI H_2O and planarians that were exposed to the same NP were combined into 1.5mL Tubes. The planarians were homogenized in 200µl of PBS using a disposable polypropylene pestle and poured into PBS glass vial with 15ml of PBS. The vial was vortexed and 120-150µl of suspension was aliquoted into each well the 96 wells of the EcoPlate™. The plate was incubated at room temperature (25°) and had its absorbance measured at 590nm every 24 hours for 6 days.

Microbiome Analysis

After exposer to MCNPs the 1.5 ml microcentrifuge tubes, which contain the planarians and their respected MCNPs, had the APW removed from the tube. 1ml of sterile APW was introduced into the microcentrifuge tube to rinse the planarian with DI H_2O to remove of any remaining MCNPs. The planarian was then placed into a new sterile 1.5 ml microcentrifuge tube. This was done to the remaining planarian and the replicates were combined into the same microcentrifuge tube to ensure that there is enough DNA for a complete and reliable genome sequencing. The samples of planaria were frozen at -80°C with minimal APW in the tube to keep

the planarians intact. The samples were frozen to ensure that the planarians microbiome does not change while in the absence of MCNPs. The samples were then shipped on dry ice to Zymo Research Corp. (Irvine, Ca) to have the DNA analyzed using the 16S rRNA gene full-service library preparation, sequencing, and bioinformatics pipeline. Zymo sample submission forms were followed, and the samples were shipped on dry ice in 1.5ml Eppendorf tubes with the APW removed.

Statistical Analysis

The IBM® statistical program SPSS, or Statistical Package for the Social Sciences was used to measure for statistical significance between average biofilm growth per nanoparticle concentration. One-way ANOVA with Dunnett's post hoc test was used to measure significance of biofilm assays.

Results

Biofilm growth inhibition by metal containing nanoparticles

Metal containing nanoparticles specifically ZnO, CuSi, and TBCC are able to inhibit the growth of biofilms of pure culture and/or mixed community bacterial biofilms. Depending on the type of nanoparticle used we observed varying degrees of biofilm inhibition. Zinc Oxide MCNPs inhibited both the pure culture bacterial biofilm of *Staphylococcus aureus* (Figure 7) and the mixed community biofilm of the plastic-adherent biofilm (Figure 5 and 6). In figure 3 the *S. aureus* biofilm was fully inhibited when exposed to 0.3 mg/ml of ZnO NPs and was shown to have a negative correlation with ZnO NP concentration. Figure 5 displays the mixed community biofilm having significant inhibition at ZnO NP concentration of 0.25 mg/ml and a negative correlation with NP concentration. The selected mix biofilm, shown in figure 6 had significant inhibition at 0.50 and 1 mg/ml of ZnO NPs. There was also the negative correlation trend present and a prominent drop in biofilm presence from concentrations of 0.15 and 0.25.

CuSi NP inhibited the selected mixed community biofilm and pure culture of *S. aureus* F-182. In figure 8 CuSi NP inhibited biofilm growth of the selected mix biofilm at almost all concentrations except for 0.15 and 0.25 mg/ml. There was significant biofilm inhibition (p-value < 0.001) at 0.50 mg/ml and complete inhibition of biofilm growth at 1 mg/ml. There was no observable trend between the growth of the selected mix biofilm and the concentration of CuSi NP. The pure culture *S. aureus* F-182 was strongly inhibited by CuSi NPs, shown in figure 9, at concentrations of 0.25, 0.50, and 1 mg/ml. The lowest concentration of 0.01 mg/ml the MCNPs had little to no effect on biofilm growth. However, the next concentrations, 0.10 and 0.15 mg/ml, showed a noticeable decrease in biofilm presence but with no statistical significance. The final three concentrations, 0.25, 0.50, 1 mg/ml, strongly inhibited biofilm growth (p-value = 0.001).

TBCC NPs were observed to have inhibitory effects on the selected mixed community biofilm (Figure 10). However, unlike ZnO and CuSi, TBCC does not seem to be able to inhibit the growth of pure culture biofilms (Figure 11). Show in figure 10 the latter concentrations of TBCC, 0.50 and 1 mg/ml, had a significant effect on the growth of the selected mixed community biofilm. The absorbance values of the concentrations that contained less than 0.50 mg/ml of MCNPs had similar values to the positive control that contained no NPs. Indicating that concentrations less than 0.50 mg/ml had little to no effect on biofilm growth. In figure 11, TBCC was not able to significantly inhibit biofilm growth of *S. aureus* F-182. All concentrations of TBCC NPs had similar non-significantly different absorbance values compared to the positive control.

Biolog EcoPlate™

Substrate utilization of the unexposed planarian microbiome showed low activity for carbohydrates, and amines and amides. Slightly higher absorbance was measured for, carboxylic and ketonic acids and for amino acids. Polymer utilization had the highest absorbance among the substrates (Figure 12). The microbiotas that have been exposed to the MCNPs follow similar patterns as described for the control. The total average well color development (AWCD) was used to visualize major differences between the control and the microbiota that have been exposed to NPs. CuSi can be seen at a higher absorbance in figure 9 however there was no statistical significance found.

Planaria *Girardia tigrina* Toxicity to MCNPs

The toxicity of MCNPs on planaria was to assess the ideal NP concentration for exposure to the microbiome without causing adverse effects or death. At concentrations of 1, 2, 5, 10, and 20 mg/ml of CuSi NPs, twitching behavior was observed when first introduced into the

suspension. CuSi NPs caused the highest mortality rate among the MCNPs with 12 planaria perishing out of 18 after a week of exposure (Figure 19). Planaria when exposed to ZnO NPs also displayed signs of toxicity by twitching when introduced to the suspension at concentrations of 2, 5, 10, and 20 mg/ml. Of the 18 planaria exposed to ZnO NPs 10 had perished after a week-long exposure (Figure 19). Planaria exposed to TBCC NPs showed no signs of toxicity and displayed normal behavior during exposure. TBCC is much less toxic compared to ZnO and CuSi due to the survival rate of the planarians exposed to TBCC NPs. Of the 18 planaria that were exposed to TBCC all 18 had survived the week-long exposure (Figure 19). A significance in mortality among planaria was found when exposed to various concentrations of CuSi NPs ($X^2 = 12.0$, $p = 0.035$) and ZnO NPs ($X^2 = 12.6$, $p = 0.027$).

Microbiome Composition of *Girardia tigrina*

The microbiome of a *Girardia tigrina* that was not exposed to MCNPs consisted mainly of Betaproteobacteria (89.5%), followed by Gammaproteobacteria (6.1%), Sphingobacteria (2.9%), Aphaproteobacteria (0.7%), and other non-classified bacteria (0.7%) (figure 14) The majority of the microbiome composition is occupied by bacteria in class Betaproteobacteria and by one species: *Pseudorhodoferax sp49091* dominating representative in the class Betaproteobacteria at 88.7% (Table 2).

As revealed by metagenomic sequencing analysis, ZnO NP exposure caused the microbiome of *Girardia tigrina to* undergo changes in its composition. There was a pronounced shift in microbial composition in favor of Gammaproteobacteria, occupying 88% of the microbiome, while Betaproteobacteria was reduced to only 3.6%. The same species prevalent in the untreated control, *Pseudorhodoferax sp49091,* was still detectable at 1.6% of Betaproteobacteria (table 2). Within Gammaproteobacteria there was no one dominating species

in the class. Sphingobacteria was not affected as much residing at 2.6% and Alphaproteobacteria was increased to a composition of 2.5% along with other classes that were uncategorized at 3%.

TBCC NPs induced limited change in the adult *Girardia tigrina* microbiome. Despite the smallest induced change compared to ZnO, and CuSi, TBCC still follows the pattern observed by ZnO NPs, regarding the two bacterial classes Betaproteobacteria and Gammaproteobacteria. Betaproteobacteria composition was decreased to 52.2% from 89.5% in the untreated control, with *Pseudorhodoferax sp49091* dominating the class with 50.7%. Conversely, Gammaproteobacteria had a composition value of 45% greater than the control that was void of NPs. Sphingobacteria's composition was at 1.1%, Alphaproteobacteria was at 0.8%, and others was found to be 0.7%.

A similar pattern of community shift observed in ZnO NP exposure was seen in CuSi NPs but not to the same magnitude. The composition of Gammaproteobacteria was increased to 48.3% from 6.1% and Betaproteobacteria was decreased to 18.7% from 89.5%. The dominant species in unexposed planaria, *Pseudorhodoferax sp49091,* was observed sharing a third of the class Betaproteobacteria at 6.3% down from 88.7% (Table 2). CuSi NPs increased the other classes of bacteria such as Sphingobacteria at 9.5% from 2.9%, Aphaproteobacteria at 9.9% from 0.7%, and other uncategorized bacteria to 12.8% from 0.7%. Unlike the other MCNPs that were used in this study, CuSi NPs stood out during this experiment by altering the diversity of the planarian microbiota.

Alpha Diversity

The microbiome of the untreated control *Girardia tigrina* was found to harbor 27 different species of microbes and had a Shannon-Weiner Index of 0.97. The Shannon-Weiner Index was used to measure diversity to better account for species richness and evenness

compared to using species richness alone to measure diversity. TBCC NPs had little to no effect on species richness and had 28 observed species (figure 15), similar to the control. However, the Shannon index for the microbiomes that were exposed to TBCC NPs was 1.64 (figure 16) which is considerably higher than the Shannon index of the control. This increase in diversity may be due to species evenness experienced by the microbiomes that were exposed to TBCC NPs which can be seen in microbial composition (table 2).

The number of metagenomically-detectable bacterial species of the microbiome varied among the planarians that were exposed to MCNPs. Paradoxically, ZnO NPs increased species richness and had 42 observed species which exceeded that of the control and TBCC NPs. By decreasing the dominant bacterial species of the microbiome other previously undetectable minor constituent species of bacteria were able to increase in abundance to above a sequencing detection threshold to contribute to the species richness of the microbiome. Exposure to ZnO NPs resulted in a Shannon index of 1.36 which is lower than the index of the microbiome exposed to TBCC NPs. Even with ZnO NPs exposure creating an environment for a greater number of species, the microbiota had 88% occupied by bacteria from the class Gammaproteobacteria. The microbiota that was exposed to TBCC NPs had only 45% occupied by Gammaproteobacteria and 52.2% in Betaproteobacteria which would result in the higher alpha diversity.

CuSi NPs increased species richness of the microbiota by a greater sum than the other MCNPs and control and was observed to have 61 species (figure 15). This substantial increase of species richness may be due to the antimicrobial properties of CuSi NPs and its ability to oxidized at a faster rate than ZnO and TBCC. The oxidation which results in the generation of ROS are able to cause more niches in the microbiome for a greater diversity. CuSi NPs are

allowing the microbiome to have more species evenness by not allowing one class dominant the entire microbiome such as with the untreated and ZnO and TBCC exposed microbiomes. Planaira microbiome exposed to CuSi NPs had only 48.3% of its microbiome occupied by Gammaproteobacteria which is the lowest number of bacteria allocated to one class when compared with the control and microbiomes exposed to ZnO and TBCC NPs (figure 14). Accounting for the substantial increase in species richness and evenness, planarian microbiomes exposed to CuSi NPs had the highest alpha diversity between the studied MCNPs with a value of 3.51 (figure 16).

Discussion

Nanoparticles Inhibited growth of Mixed and Pure Culture Biofilms

ZnO NPs at concentrations lower than 0.25 mg/ml do not have inhibitory effects on bacterial biofilms. From the conducted experiments ZnO NPs begins to show signs of inhibition when concentration of MCNPs reaches at least 0.25 mg/ml. Figure 9 shows significant biofilm inhibition of the mixed community biofilm at 0.25 mg/ml ($p < 0.001$). Figures 6 and 7 also show significant biofilm inhibition of the selected mix and *S. aureus* F-182 biofilm at concentrations greater than 0.25 mg/ml ($p < 0.001$; $p = 0.001$). ZnO NPs was best able to inhibit biofilm growth at the higher concentrations for pure cultures and for mixed community biofilms. The mixed community biofilm and the selected mix had a higher tolerance to ZnO NPs than CuSi NPs as they were able to withstand concentrations of 0.25 mg/ml and above while *S. aureus* was completely inhibited at that same concentration. This could be due to the interactions between different species of the mixed-biofilm community affecting one-another's development, structures, and functions (James *et al*., 1995; Harrison, 2007; Moons *et al*., 2009).

Throughout the study, the biomass of the mixed community biofilm was consistently greater than the biomass of the single-species biofilm, as determined by the plate reader spectrophotometer. The positive controls for the mixed biofilms had higher absorbance values than the *S. aureus* biofilm absorbance values. Lee *et al.,* 2014 also observed this phenomenon for *K. pneumoniae* (KP-1), within the mixed-species biofilm the biomass was significantly higher than of KP-1 single-species biofilm. This potentially suggests the presence of syntropy within the mixed-species biofilm that allows it to achieve higher biomass than that of the single-species biofilm. (Lee *et al*., 2014). The higher biomass the biofilm possesses the more resilient the biofilm will be toward MCNPs and the lower the MCNPs to cell ratio. The microbial physiology

of the mixed community biofilm equips it with the ability to become a more resilient biofilm compared to a single-species biofilm.

This study exposed NPs to biofilm-forming microbial communities in the exponential phase of growth. ZnO NPs was effective against mixed and pure culture bacterial biofilms at the exponential growth phase. However, it has been previously observed that the antibacterial properties of nanoparticles are significantly decreased at the lag and stationary phases (Dadi *et al*., 2019). This may be reflection of ZnO NPs ability to disturb the process of bacterial DNA amplification (Li *et al.,* 2010). If ZnO NPs are disturbing the process of DNA amplifications, then we should see inhibition during growth phases, when DNA amplification is at its highest, as was demonstrated in this study. This was also demonstrated by (Kaur *et al.,* 2021) when they described ZnO NPs inhibiting bacterial adhesion to glass, plastic, and aluminum.

Copper Silicon NPs were able to reduce biofilm growth of both pure culture and mixed community bacterial biofilms at the higher concentrations and the lower concentrations as well. This can be seen in figures 8 and 9, the biofilm presence was more similar among most of the concentrations, resulting them having no observable trend. However, in the cases of ZnO NPs there was an observable trend between the NP concentrations and biofilm presence. Indicating that ZnO has more inhibitory potential at high concentrations of 0.50 mg/ml or above, whereas CuSi can be toxic at lower levels and may not be dose dependent below 1 mg/ml.

CuSi NPs ability to inhibit biofilms at low concentrations of 0.25 mg/ml or below may be due to certain antimicrobial properties that copper holds. Cu undergoes oxidation more easily than other metals (Bahadar *et al.,* 2016; Struder *et al.,* 2010) and Cu NPs dissolves and releases ions into the surroundings faster than other noble metals (Sánchez-López *et al*., 2020). The presence of metal oxide NPs and its ions induce the generation of ROS and increase their

concentration within the cell. The copper mediated increase in ROS subject the cell to oxidative stress and can lead to apoptosis (Applerot *et al.,* 2012). The combination of faster ion release and easier oxidation is what leads CuSi NPs to have more inhibitory effect of biofilms at lower concentrations compared to ZnO and TBCC NPs.

In the case of the selected mixed community biofilm TBCC was able to inhibit biofilm growth at 0.50 mg/ml and 1.00 mg/ml (figure 10). Both concentrations inhibited the growth of the biofilm by the same magnitude as there was not significant difference in absorbance value between the two concentrations. There was no observable pattern following the increase of NP concentrations and absorbance values in figure 10. Against the pure culture *S. aureus* TBCC NPs showed no signs of inhibitory effects against biofilm formation. In figure 7 it shows that the positive control along with all concentrations of TBCC had similar absorbance values displaying no inhibitory effects at any concentration ($p = 0.003$, error bars overlap). TBCC NPs were not able to inhibit the growth of the pure culture *S. aureus* biofilm at any level of NP concentration.

Biofilm formers that were exposed to TBCC did not experience inhibition at the same level as biofilm formers at were exposed to ZnO or CuSi NPs. This may be due to the fact that TBCC is a less reactive and less destructive form of Cu when compared to copper sulfate (CS) (Zheng *et al.,* 2018). TBCC is low in toxicity, compared to CS, and has a high antioxidant potential (Yu *et al.,* 2021). MCNPs antimicrobial properties reside within their ability to induce the generation of ROS that cause oxidative stress within the cell. This can only happen if the rate of ROS production overrides the rate of ROS removal and if TBCC NPs are exhibiting antioxidant properties than the microbes being exposed to TBCC NPs may not reach the requisite concentration to induce lethal oxidative stress.

Biolog EcoPlate™

Substrate utilization of the planarian microbiota showed no significant difference to the microbiota that have been exposed to MCNPs. The experiment used 0.10 mg/ml of MCNPs to expose the planarians and at this concentration no differences were found in the substrate utilization. It may be ideal to run an experiment using higher concentrations of MCNPs; however, the risk of killing the planarians would be introduced. The challenge was to find a concentration where all planarians survived 1 week of exposure to a NP type.

MCNPs Toxicity on planaria

Planaria exposed to ZnO and CuSi showed signs of toxicity and ultimately perished when the suspension was at least 1 mg/ml of MCNPs. CuSi showed higher levels of toxicity than ZnO or TBCC by having 12 of the 18 exposed to CuSi NPs perish (Figure 19). This could be due to the elemental nature of copper and how readily it oxidizes generating more ROS than ZnO and TBCC. Planaria when exposed to ZnO or CuSi NPs have a dose dependent response (Table 4). However, unlike CuSi when ZnO concentrations reached 20 mg/ml the planarians survived the weeklong exposure period. Behaviorally, TBCC did not affect the planaria in a negative manner such as was observed with ZnO and CuSi. TBCC was the safest MCNP to the planaria *Girardia tigrina* in terms of mortality. Shown in figure 19 all of the planaria from all concentrations of TBCC survived the week-long exposure. This may be due to the less reactive and less destructive form of copper and how oxidation may not happen as readily as CuSi (Zheng *et al*, 2018). ZnO and CuSi used in this study have shown promise as a toxic agent to the planaria *G. tigrina.* Further toxicology studies will need to be conducted to confirm ZnO toxic properties at concentrations ≥ 20 mg/ml and to confirm TBCC NPs nontoxicity to planaria.

Microbiome Composition Shifted in Presence of Nanoparticles

The majority of the control bacterial flora from the *Girardia tigrina* planarian microbiome belonged to the class of Betaproteobacteria 89.5% specifically, the species *Pseudorhodoferax sp49091.* Bijnens *et al.*, 2021 reported similar results when studying the microbiome of the planarian *S. mediterranea*, stating that the microbiomes consisted mainly of Betaproteobacteria before exposure to Ag NPs. Gammaproteobacteria was the other significant class of bacteria found comprising 6.1% in the control microbiome. When exposed to ZnO, CuSi, or TBCC NPs the planarian microbiome experienced a shift in its community composition as determined by metagenomic sequence analysis. This shift was mainly between two classes of bacteria found in the planarian microbiota: Betaproteobacteria and Gammaproteobacteria. Interestingly, all MCNPs decreased the abundance of bacteria belonging to the class Betaproteobacteria and increased the abundance of bacteria belonging to the class Gammaproteobacteria. ZnO NPs had the most pronounced decrease in Betaproteobacteria (-85.9%) and the most pronounced increase in Gammaproteobacteroa (+81.9%).

CuSi NPs decreased Betaproteobacteria (-70.8%) and increased Gammaproteobacteria (+42.2%) but not to the magnitude of ZnO. CuSi instead facilitated a more diverse microbiome compared to ZnO or TBCC. Sphingobacteria (+6.6%), Alphaproteobacteria (+9.2%), and Others (+12.1%) had increased more in the presence of CuSi NPs than in the presence of the other NPs. This profound increase of diversity may be due to the fact that the class Gammaproteobacteria is the most diverse class of gram-negative bacteria. However, ZnO NPs increased their Gammaproteobacteria class to a much higher percentage compared to CuSi NPs and had only the second largest diversity from this study. CuSi NP treatment appeared to increase diversity by

increasing the abundance of other classes such as, Alphaproteobacteria, Sphingobacteriia, and other unspecified classes (table 16).

The planarian microbiome that had been exposed to TBCC NPs had a shift in community composition that was more similar to the microbiome of the untreated control than the microbiome exposed to ZnO NPs or CuSi NPs. Betaproteobacteria (-37.3%) decreased and Gammaproteobacteria (+38.9%) increased exhibiting the smallest shift compared to ZnO NPs and CuSi NPs. *Pseudorhodoferax sp49091* remained the dominate species in the class Betaproteobacteria following exposure to TBCC NPs.

In the present study, it was found that MCNP exposure can decrease the relative abundance of Betaproteobacteria in *G. tigrina* while increasing the relative abundance of Gammaproteobacteria. This shift in microbial community composition of the microbiome was also observed with other species of planaria. When exposed to microplastics a microbial shift in the microbiome was experienced by *D. japonica*. The abundance of Proteobacteria and Bacteroidetes decreased while the relative abundance of Firmicutes, Actinobacteria, and Acidobacteria increased (Han *et al.*, 2022). When *S. mediterranea* was exposed to Ag NPs the relative abundance of Proteobacteria and Bacteroidetes decreased in favor of Firmicutes, Actinobacteria and Acidobacteria (Bijnens *et al.*, 2021). As we learn more about the microbiome and its importance it is crucial, that we understand how certain materials, such as NPs, may alter the microbiome. Investigating the planarian microbiome such as *G. tigrina* may help us understand more about the microbiome and how the composition and diversity play a role in the organisms' health.

Figures

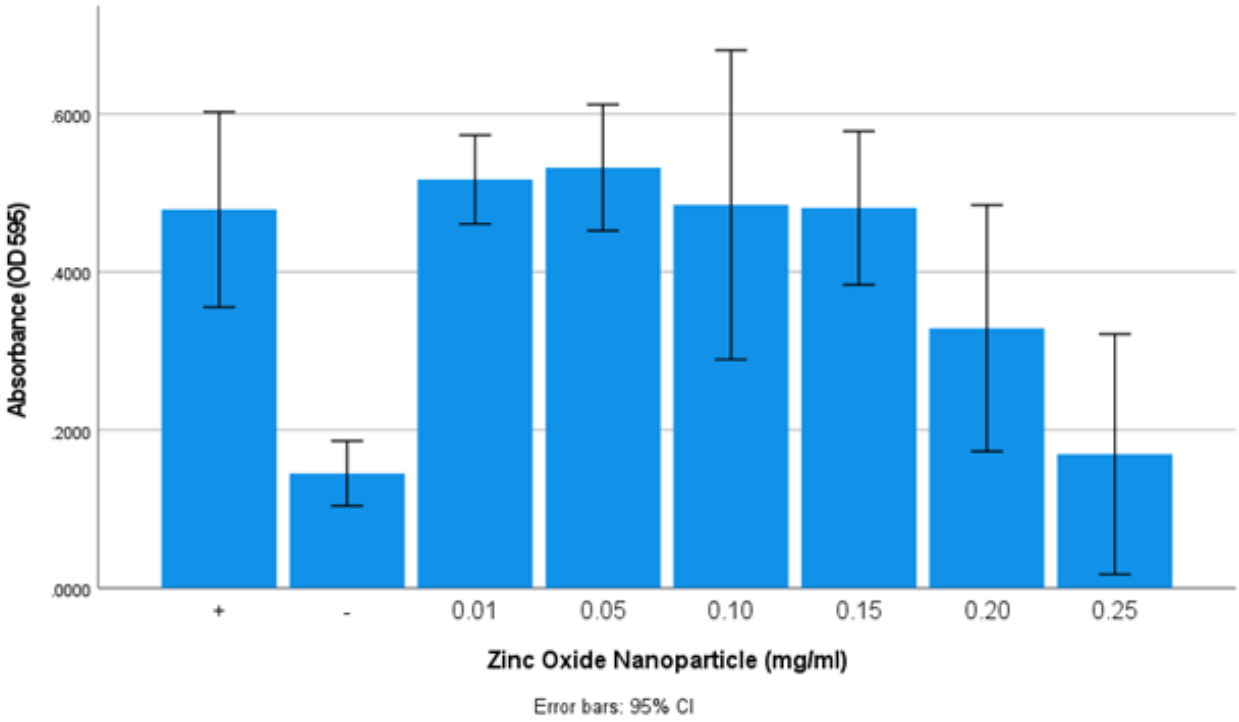

Figure 5. Mixed community biofilm growth in various concentrations of Zinc Oxide nanoparticles over a 24-hour period. Mixed community biofilm formation is dependent on the nanoparticle concentration. Nanoparticle concentrations of 0.25 mg/ml had significant decreasing effects on biofilm formation ($F = 18.744$, $p < 0.001$). One-way ANOVA performed. Normally distributed residuals ($W = 0.953$, $p = 0.392$) with equal variances ($p = 0.217$).

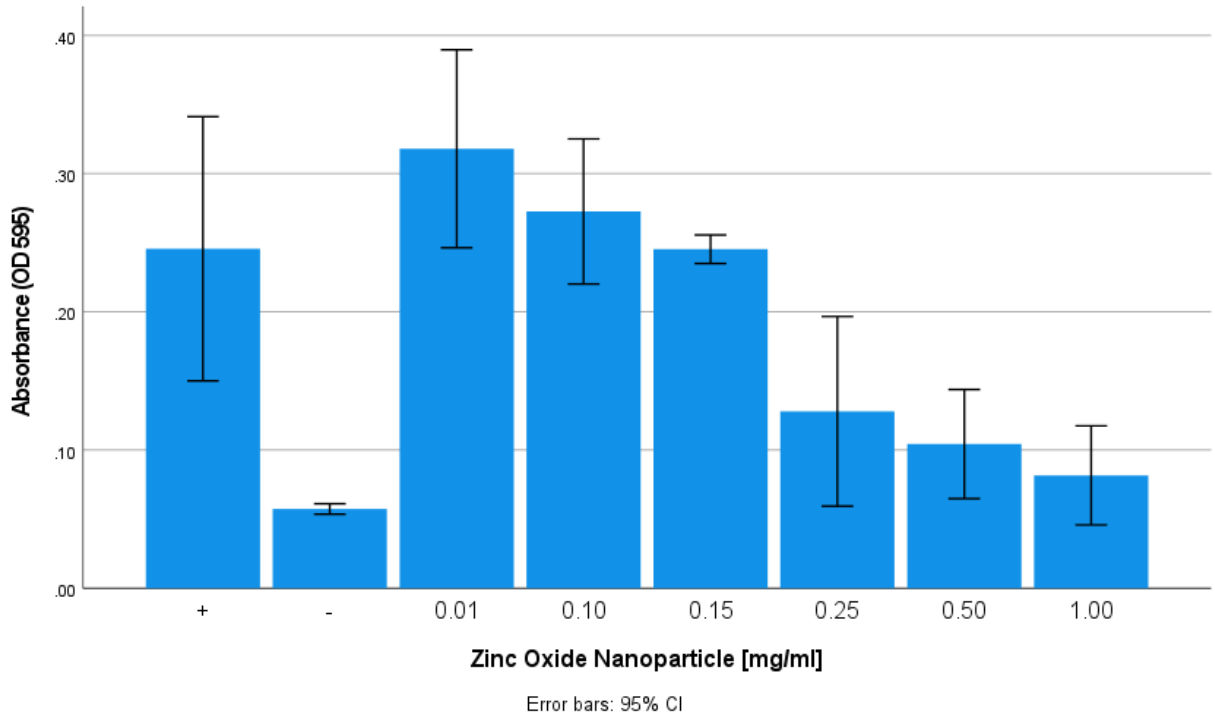

Figure 6. Selected Mixed community biofilm growth measured in various concentrations of Zinc Oxide MCNPs over a 24-hour period. Selected Mixed community biofilm formation is dependent on the ZnO NP concentration. NP concentrations of 0.50 and 1.0 mg/ml had a significant negative effect on biofilm growth ($F = 45.225$, $p < 0.001$). One-way ANOVA performed. Normally distributed residuals ($W = 0.927$, $p = 0.118$) with equal variances ($p = 0.072$).

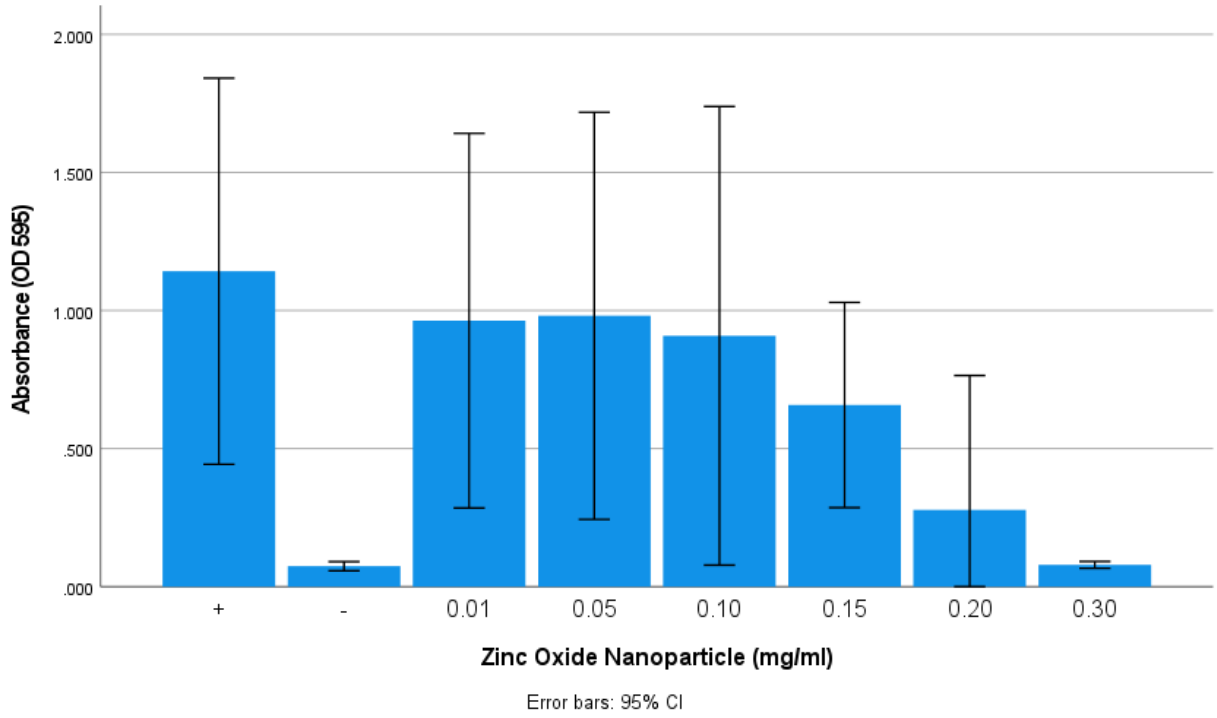

Figure 7. *S. aureus* strain F-182 biofilm measured in various concentrations of Zinc Oxide MCNPs over a 24-hour period. *S. aureus* strain F-182 biofilm formation is dependent on the ZnO NP concentration. ZnO NPs inhibited biofilm formation at concentration 0.3 mg/ml ($F = 8.032$, $p = 0.001$). One-way ANOVA performed. Normally distributed residuals ($W = 0.946$, $p = 0.290$) with equal variances ($p = 0.357$).

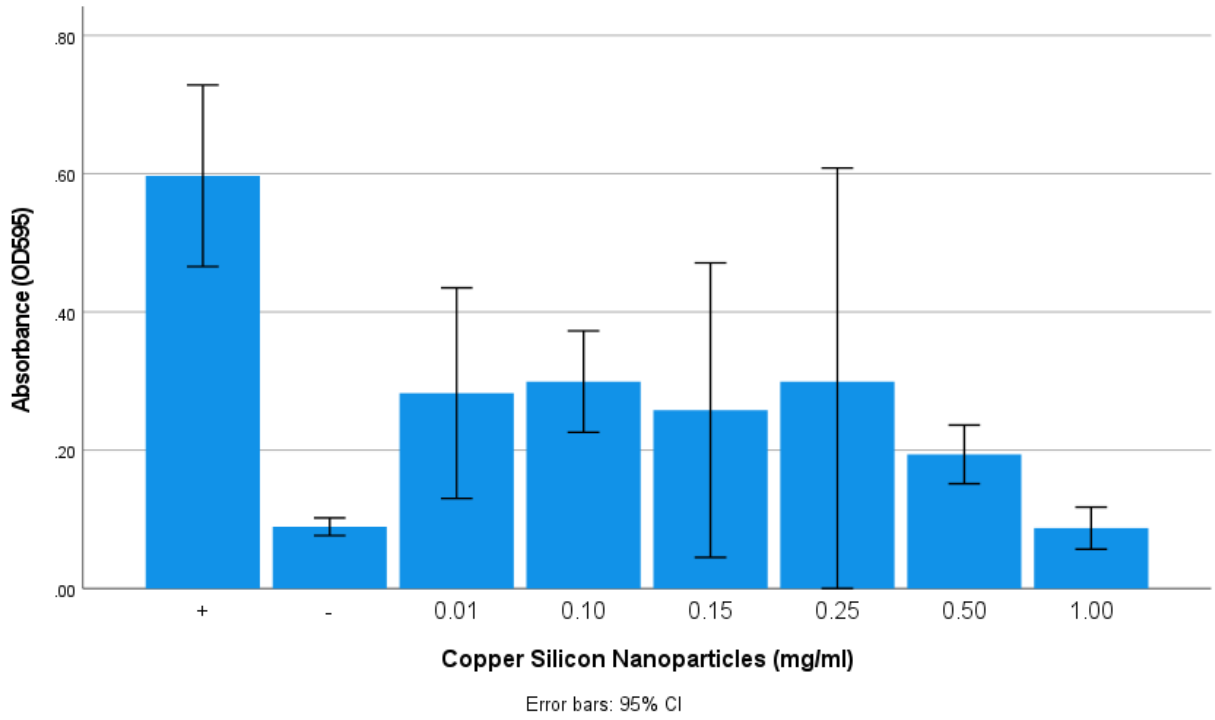

Figure 8. Selected Mixed community biofilm growth measured in various concentrations of Copper Silicon NPs over a 24-hour period. Selected Mixed community biofilm formation is dependent on the CuSi NP concentration. NP concentrations of 0.01, 0.10, 0.50 and 1.0 mg/ml had a significant negative effect on biofilm growth ($F = 16.629$, $p < 0.001$). One-way ANOVA performed. Normally distributed residuals ($W = 0.935$, $p = 0.176$) with equal variances ($p = 0.009$).

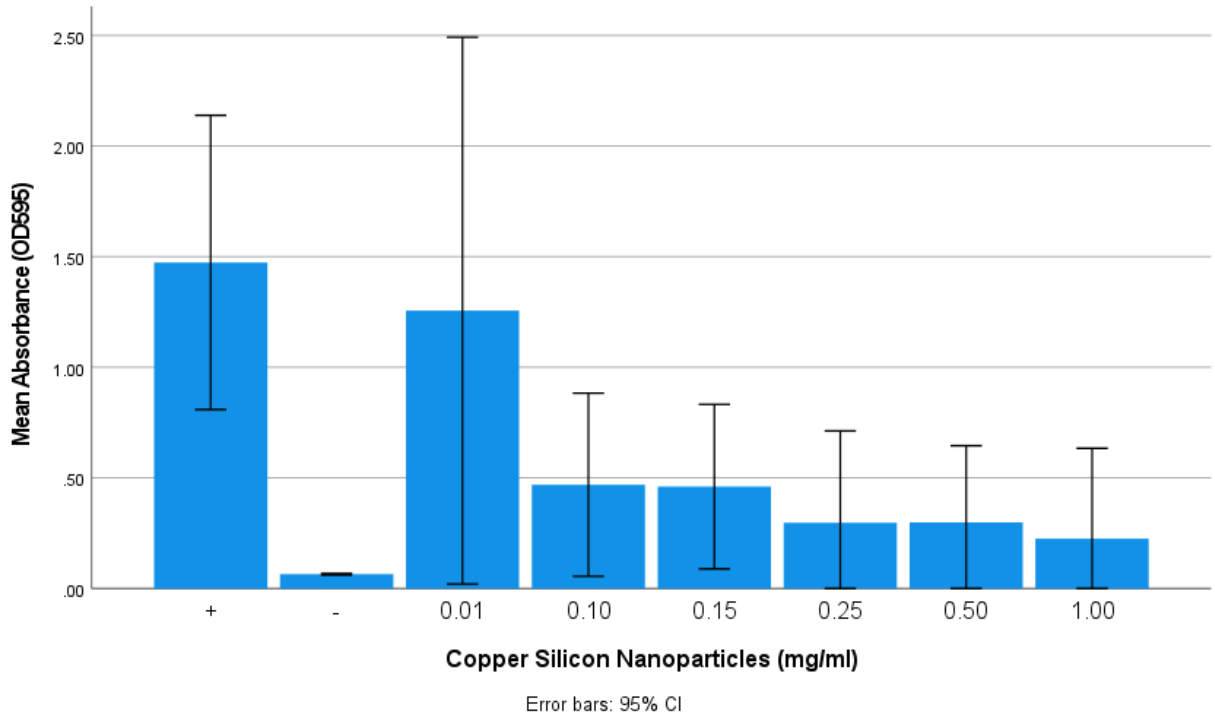

Figure 9. *S. aureus* strain F-182 biofilm growth measured in various concentrations of Copper Silicon NPs over a 48-hour period. *S. aureus* strain F-182 biofilm formation is dependent on the CuSi NP concentration. Copper Silicon Nanoparticles inhibits biofilm formation of *S. aureus* strain F-182 ($F = 8.230$, $p = 0.001$). NP concentrations of 0.25, 0.50, and 1.00 mg/ml significantly inhibits biofilm formation.

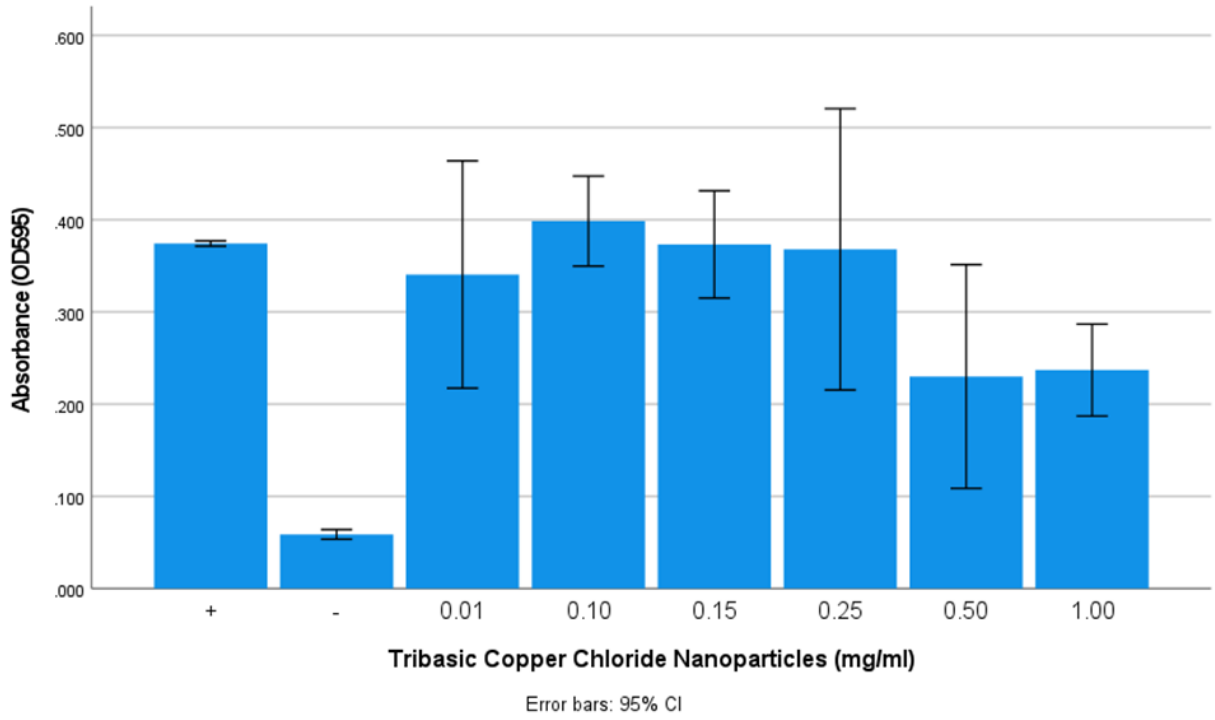

Figure 10. Selected Mixed community biofilm in varies concentrations of Tribasic Copper Chloride NPs over a 24-hour period. Various concentrations of TBCC NPs had a significant inhibitory effect on the biofilm formation ($F = 10.093$, $p < 0.001$). NP concentrations of 0.50 and 1.00 mg/ml had the greatest inhibitory effect.

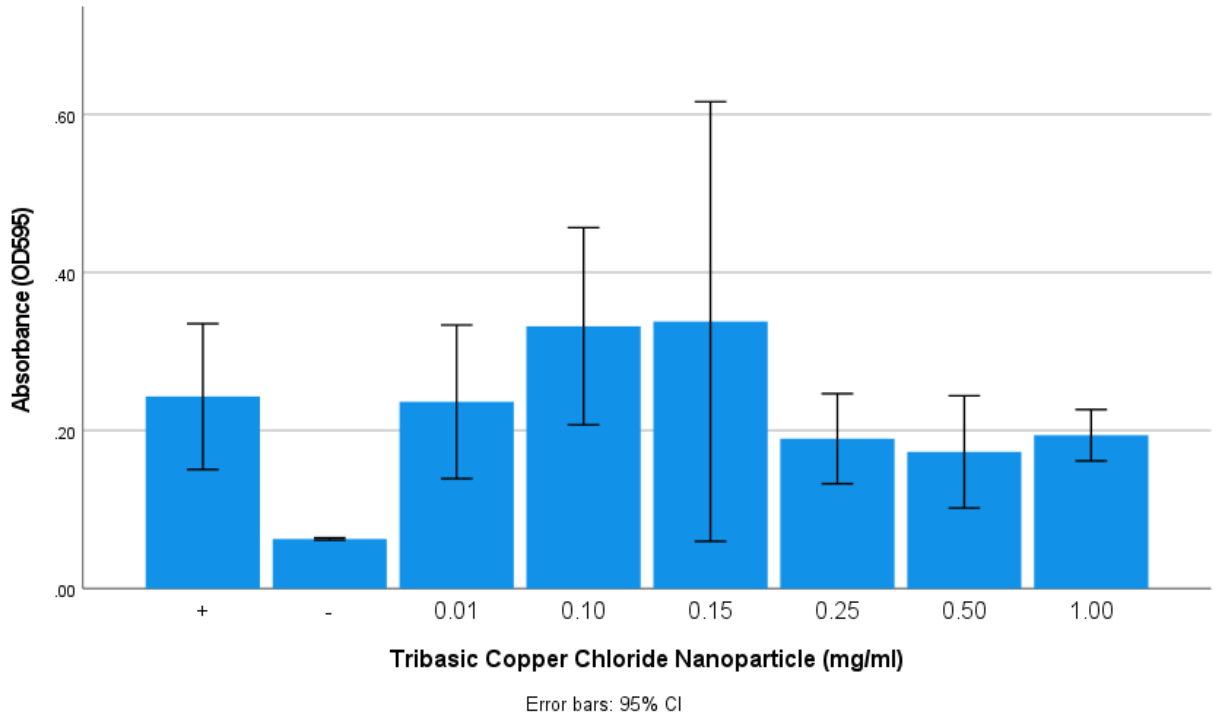

Figure 11. *S. aureus* strain F-182 biofilm growth measured in various concentrations of Tribasic Copper Chloride NPs over a 24-hour period. *S. aureus* strain F-182 biofilm formation is not dependent on the TBCC NP concentration. TBCC NPs had no significant inhibitory effects on biofilm formation of *S. aureus* strain F-182 ($F = 6.007$, $p = 0.003$).

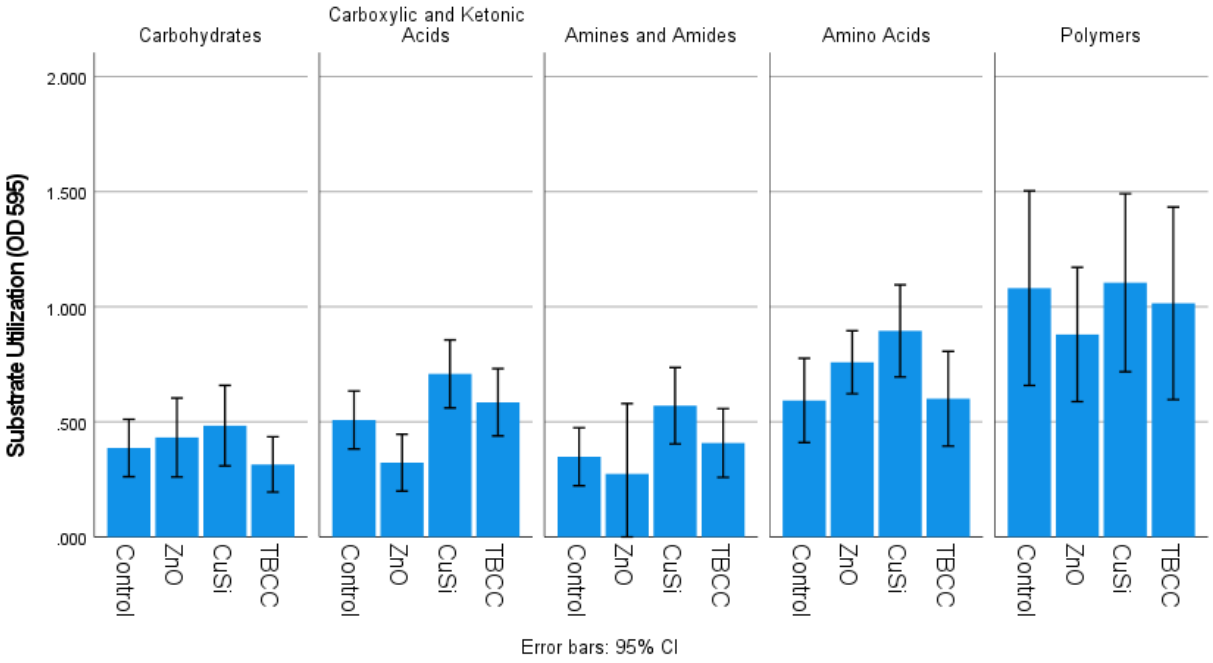

Figure 12. Mean of substrate utilization of carbon substrates from different substrate groups by Planarian microbial flora based on 168-h incubation (n=3). The error bars dictate that no significance was found in substrate utilization between the microbes exposed to NPs. Substrate grouping breakdown can be found in Table 3.

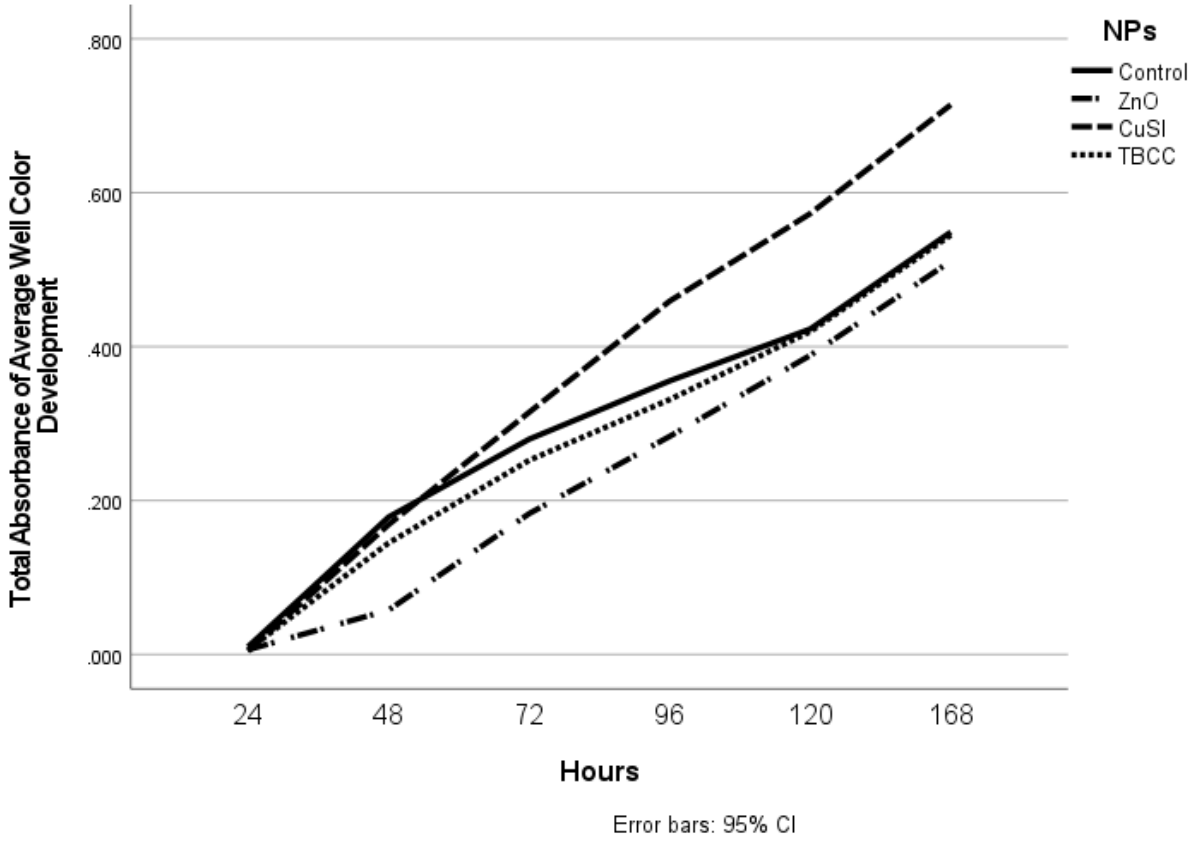

Figure 13. Biolog EcoPlate™ Total Average Well Color Development (AWCD) of microbiota flora from exposed *Girardia tigrina*, incubated over 168 hours. Made to visualize major differences between total absorbance of microbiota flora and the effects of MCNPs of the total AWCD. There is no significant difference between total AWCD of the tested NPs. Shapiro-Wilk: ($W = 0.975$, $p = 0.780$). Levenes statistic: ($p = 0.780$). One-Way Anova: ($F = 0.414$, $p = 0.745$)

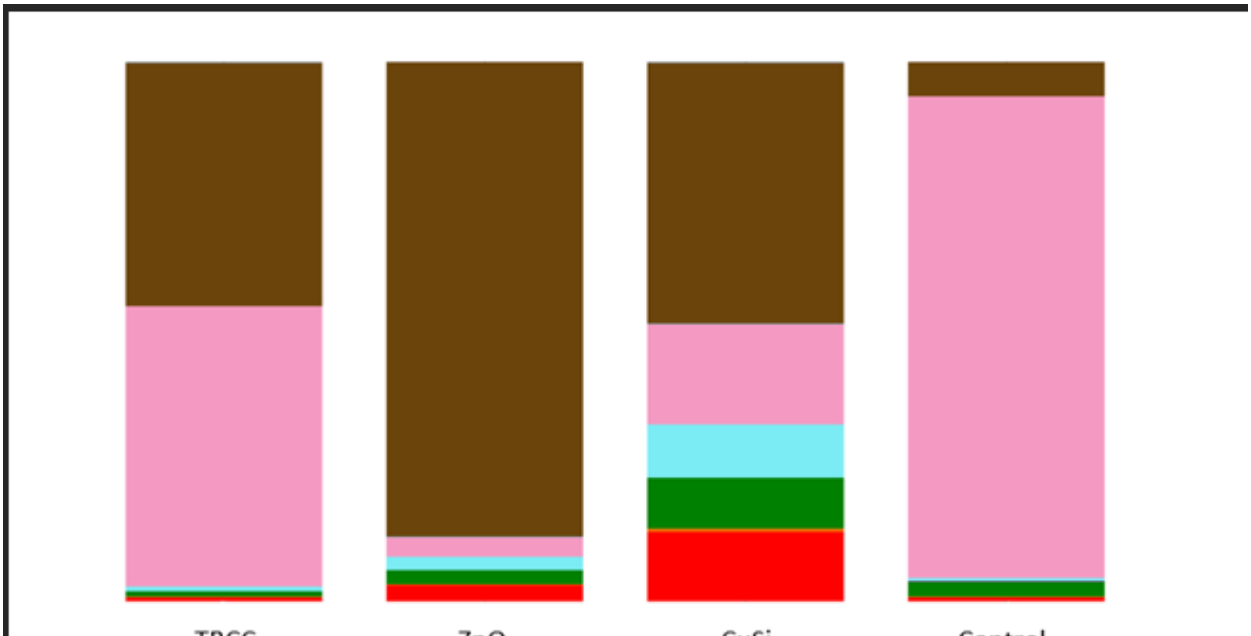

Legend	Taxonomy	Total %	TBCC %	ZnO %	CuSi %	Control.Void.of.NPs %
	None;Other;Other	4.3%	0.7%	3.0%	12.8%	0.7%
	k__Bacteria;p__Actinobacteria;c__Actinobacteria	0.1%	0.1%	0.0%	0.1%	0.0%
	k__Bacteria;p__Bacteroidetes;c__Cytophagia	0.2%	0.1%	0.1%	0.5%	0.1%
	k__Bacteria;p__Bacteroidetes;c__Sphingobacteriia	4.0%	1.1%	2.6%	9.5%	2.9%
	k__Bacteria;p__Chlamydiae;c__Chlamydiae	0.0%	0.0%	0.0%	0.0%	0.0%
	k__Bacteria;p__Firmicutes;c__Bacilli	0.0%	0.0%	0.0%	0.0%	0.0%
	k__Bacteria;p__Proteobacteria;c__Alphaproteobacteria	3.4%	0.8%	2.5%	9.9%	0.7%
	k__Bacteria;p__Proteobacteria;c__Betaproteobacteria	41.0%	52.2%	3.6%	18.7%	89.5%
	k__Bacteria;p__Proteobacteria;c__Deltaproteobacteria	0.0%	0.0%	0.1%	0.1%	0.0%
	k__Bacteria;p__Proteobacteria;c__Gammaproteobacteria	46.9%	45.0%	88.0%	48.3%	6.1%
	k__Bacteria;p__Spirochaetae;c__Spirochaetes	0.0%	0.1%	0.0%	0.1%	0.0%

Figure 14. Microbial Composition by Class. Taxa composition plots illustrate the microbial composition at different taxonomy levels from phylum to class.

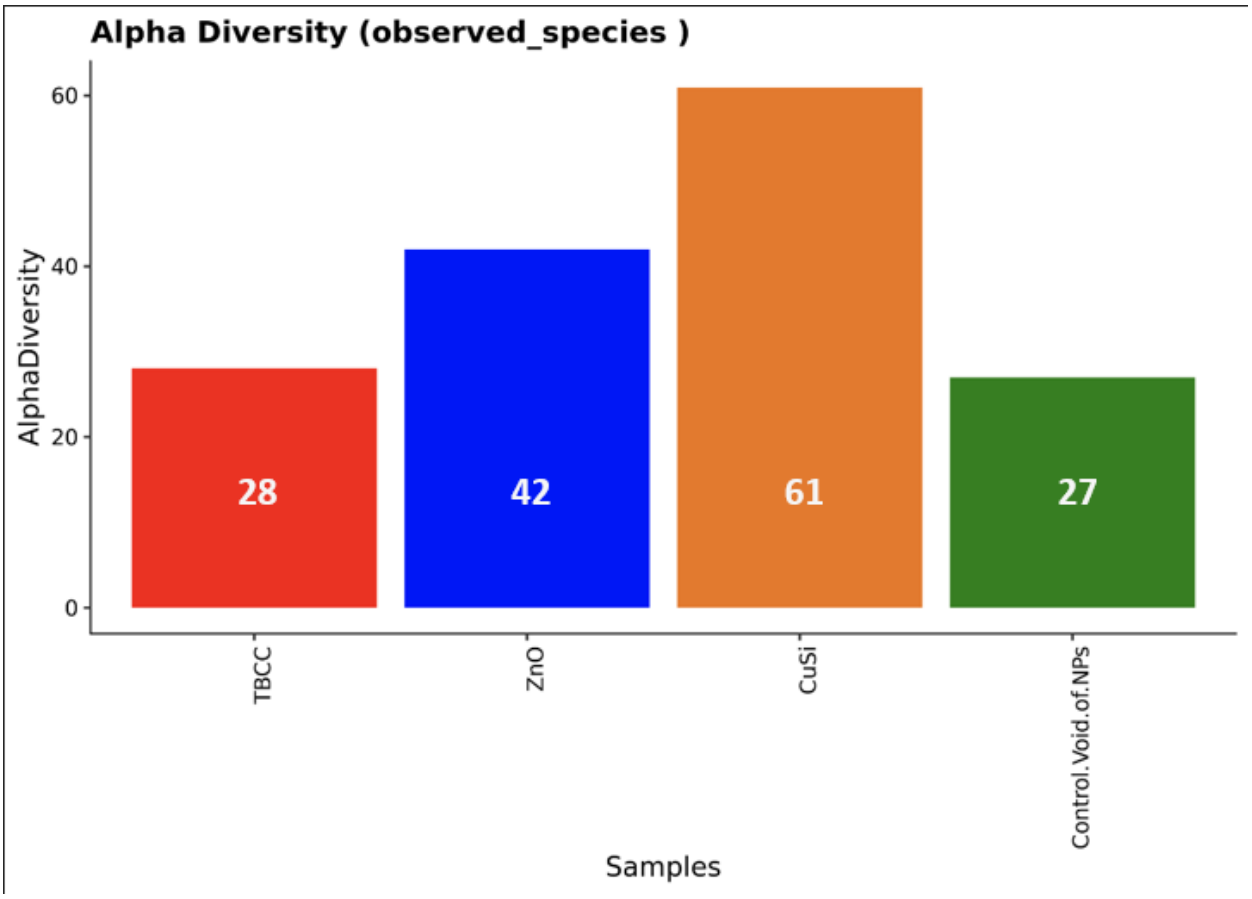

Figure 15. Alpha Diversity Histogram Plot of observed number of species.

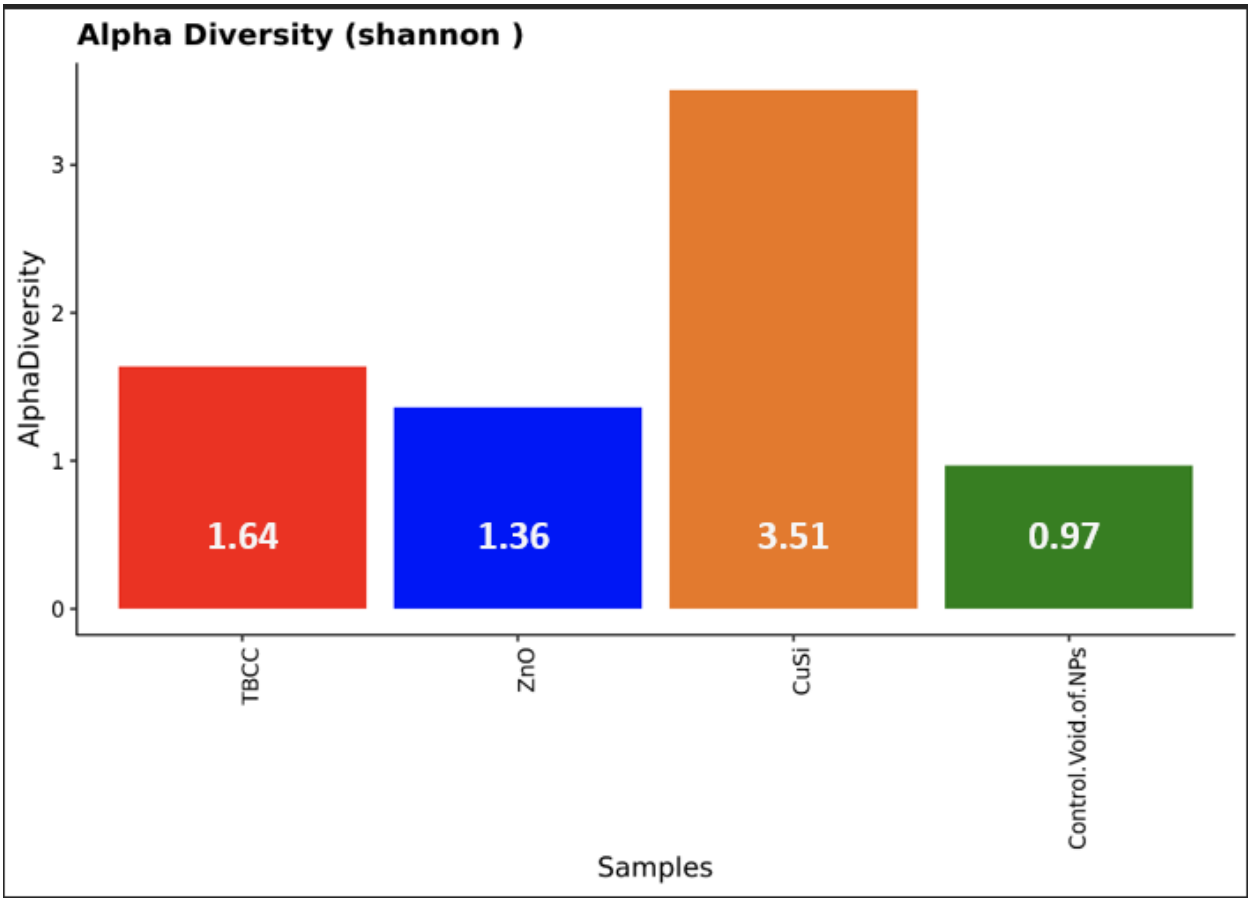

Figure 16. Alpha Diversity Histogram Plot using the Shannon-Weiner index. CuSi has displayed the highest diversity with a Shannon index of 3.5. Although ZnO has accounted for a higher number of observed species TBCC has a higher Shannon index of ~1.5 when accounting for species richness and evenness. Shannon index values taken from Figure 13.

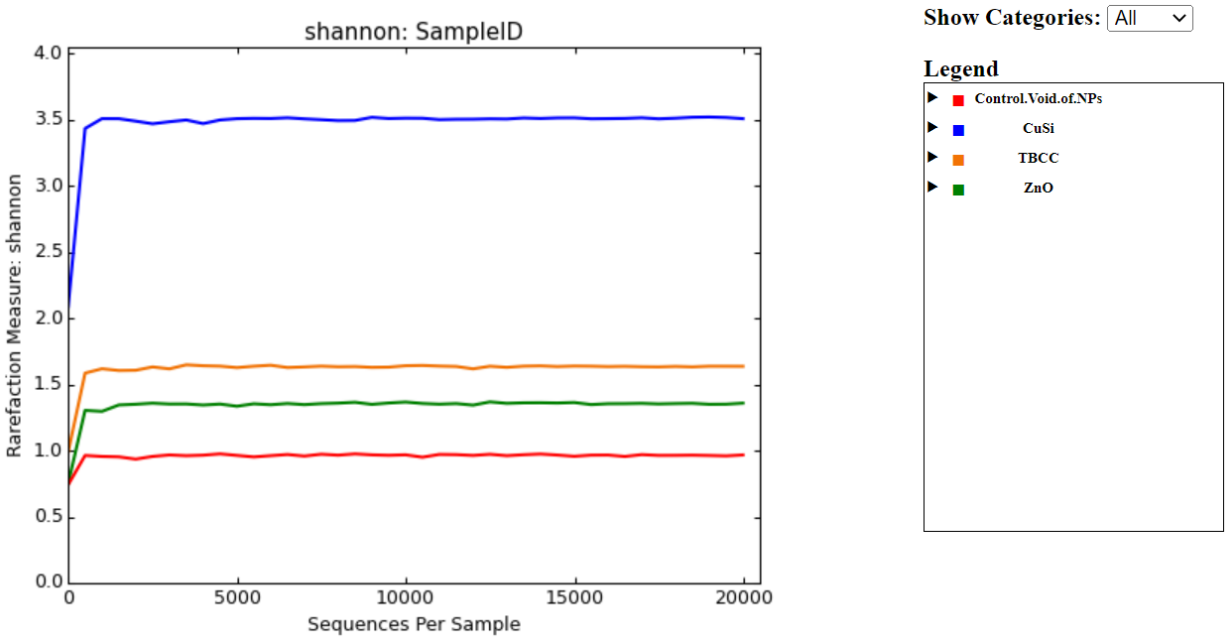

Figure 17. Alpha Diversity (Shannon–Wiener) Rarefraction Plots

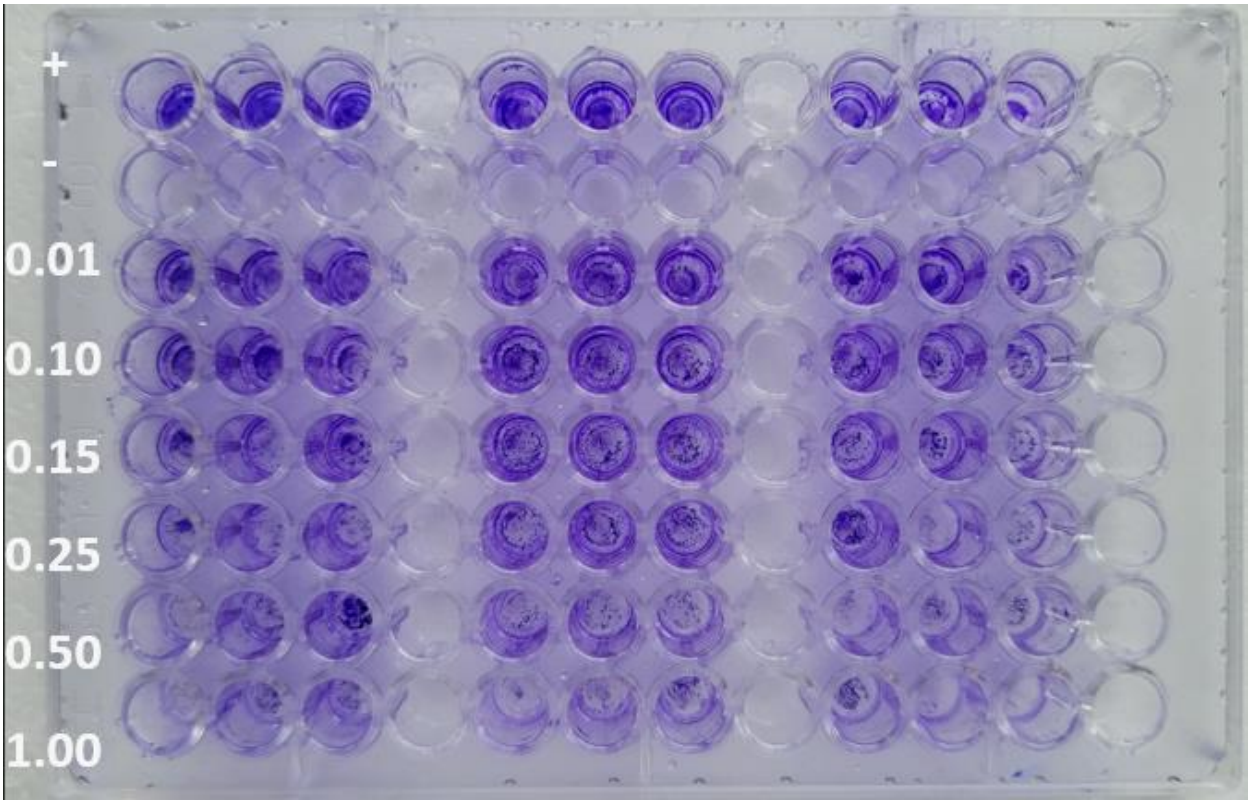

Figure 18. Mix Biofilm grown in a 96 MWP with various concentrations of CuSi NPs (mg/ml)

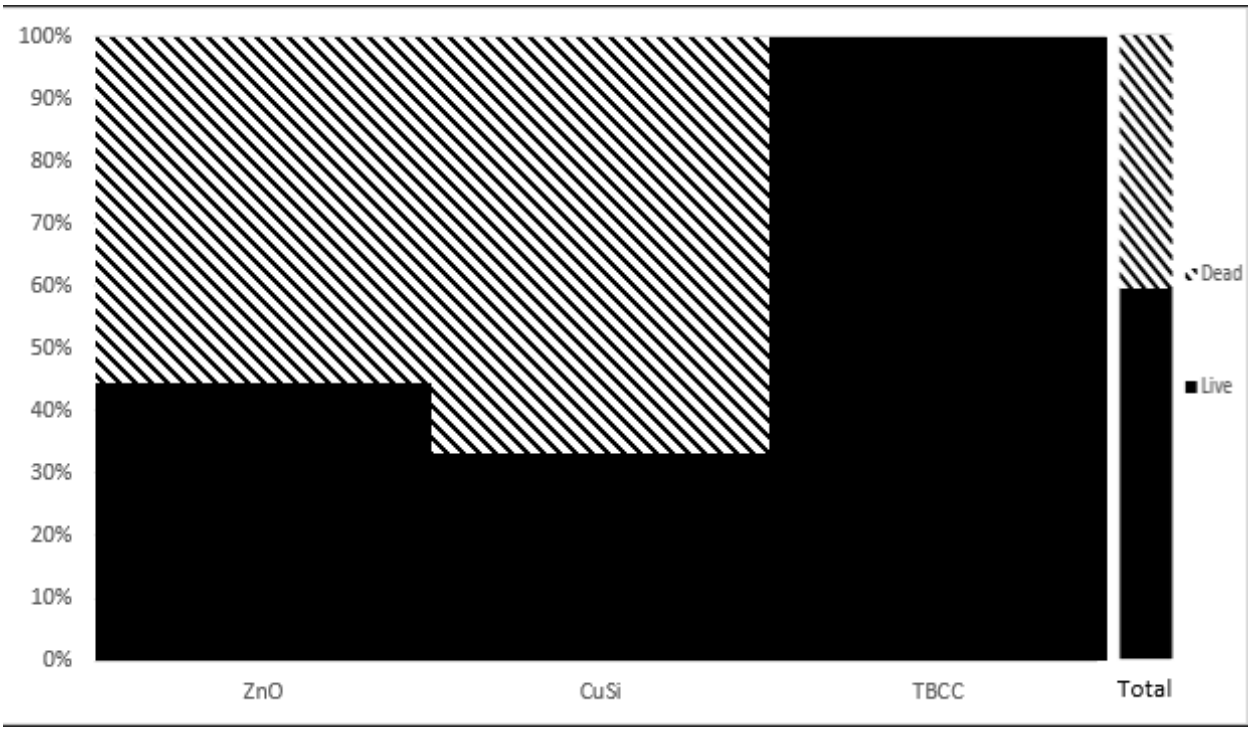

Figure 19. Mosaic chart reporting mortality status of all planaria after week-long exposure to various concentrations of MCNPs. Sample sizes of 18 planaria per MCNP type. There is a significance in mortality when planaria are exposed to MCNPs. (ZnO NPs: $X^2 = 12.6$, $p = 0.027$; CuSi NPs: $X^2 = 12.0$, $p = 0.035$). TBCC has no statistics due to the values being constant.

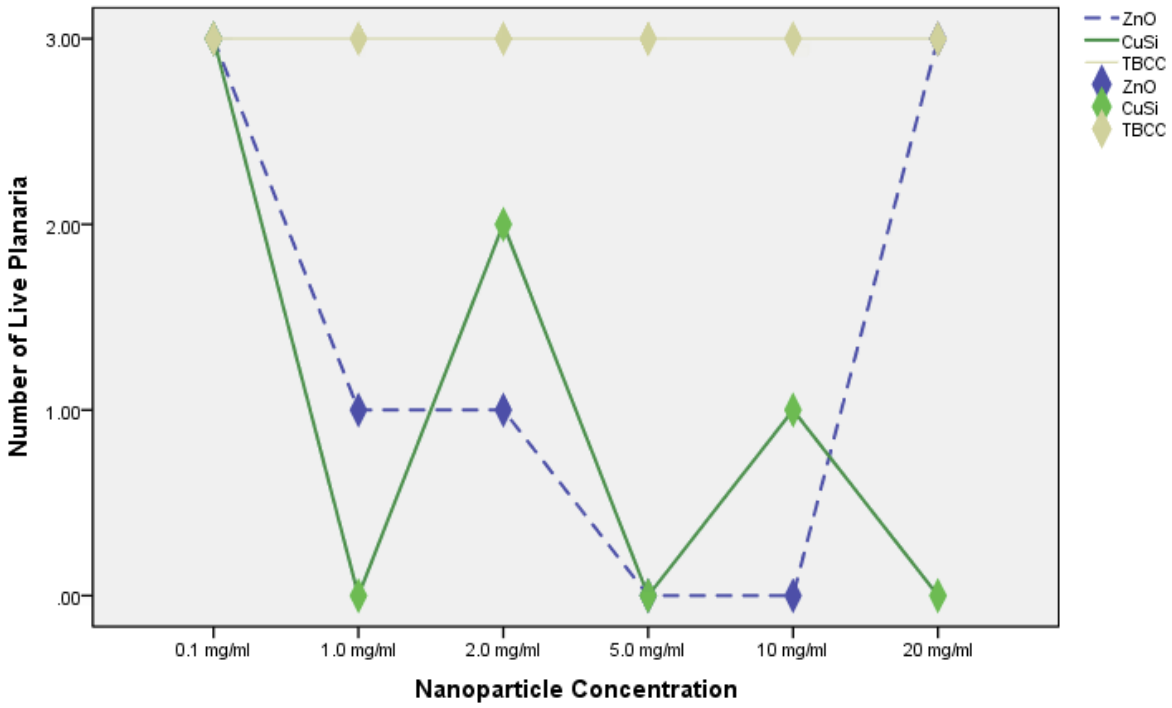

Figure 20. MCNPs and planarian dose dependent toxicity study. ZnO (X^2 = 12.6 p = 0.027); CuSi (X^2 = 12.0 p = 0.035)

Tables

Legend	Taxonomy	Total %	TBCC %	ZnO %	CuSi %	Control.Void.of.NPs %
	None;Other;Other;Other;Other;Other;Other	4.3%	0.7%	3.0%	12.8%	0.7%
	k__Bacteria;p__Actinobacteria;c__Actinobacteria;o__Corynebacteriales;f__Nocardiaceae;g__Rhodococcus;s__erythropolis-qingshengii-sp5959	0.0%	0.1%	0.0%	0.0%	0.0%
	k__Bacteria;p__Actinobacteria;c__Actinobacteria;o__Micrococcales;f__Micrococcaceae;g__Kocuria;s__assamensis-palustris	0.0%	0.0%	0.0%	0.1%	0.0%
	k__Bacteria;p__Bacteroidetes;c__Cytophagia;o__Cytophagales;f__Cytophagaceae;g__Arcicella;s__aurantiaca	0.0%	0.0%	0.0%	0.0%	0.0%
	k__Bacteria;p__Bacteroidetes;c__Cytophagia;o__Cytophagales;f__Cytophagaceae;g__NA;s__sp15459	0.1%	0.0%	0.0%	0.2%	0.0%
	k__Bacteria;p__Bacteroidetes;c__Cytophagia;o__Cytophagales;f__Cytophagaceae;g__Pseudarcicella;s__sp15329	0.1%	0.1%	0.1%	0.3%	0.1%
	k__Bacteria;p__Bacteroidetes;c__Sphingobacteriia;o__Sphingobacteriales;f__Chitinophagaceae;g__Chitinophaga;s__soli	0.3%	0.1%	0.1%	1.1%	0.0%
	k__Bacteria;p__Bacteroidetes;c__Sphingobacteriia;o__Sphingobacteriales;f__Chitinophagaceae;g__Taibaiella;s__chishuiensis	0.0%	0.0%	0.0%	0.2%	0.0%
	k__Bacteria;p__Bacteroidetes;c__Sphingobacteriia;o__Sphingobacteriales;f__Chitinophagaceae;g__Taibaiella;s__sp18320	0.8%	0.6%	0.0%	1.1%	1.6%
	k__Bacteria;p__Bacteroidetes;c__Sphingobacteriia;o__Sphingobacteriales;f__Sphingobacteriaceae;g__Pedobacter;s__duraquae	0.1%	0.0%	0.6%	0.0%	0.0%
	k__Bacteria;p__Bacteroidetes;c__Sphingobacteriia;o__Sphingobacteriales;f__Sphingobacteriaceae;g__Pedobacter;s__ginsengisoli	0.3%	0.2%	0.2%	0.4%	0.2%
	k__Bacteria;p__Bacteroidetes;c__Sphingobacteriia;o__Sphingobacteriales;f__Sphingobacteriaceae;g__Pedobacter;s__koreensis	0.8%	0.1%	0.3%	2.0%	0.9%
	k__Bacteria;p__Bacteroidetes;c__Sphingobacteriia;o__Sphingobacteriales;f__Sphingobacteriaceae;g__Pedobacter;s__nyackensis-steynii-trunci	1.5%	0.1%	1.0%	4.6%	0.1%
	k__Bacteria;p__Bacteroidetes;c__Sphingobacteriia;o__Sphingobacteriales;f__Sphingobacteriaceae;g__Pedobacter;s__nyackensis-trunci	0.1%	0.0%	0.0%	0.2%	0.0%
	k__Bacteria;p__Bacteroidetes;c__Sphingobacteriia;o__Sphingobacteriales;f__Sphingobacteriaceae;g__Pedobacter;s__steynii	0.1%	0.0%	0.4%	0.0%	0.0%
	k__Bacteria;p__Chlamydiae;c__Chlamydiae;o__Chlamydiales;f__Simkaniaceae;g__*Rhabdochlamydia;s__sp19953	0.0%	0.0%	0.0%	0.0%	0.0%
	k__Bacteria;p__Firmicutes;c__Bacilli;o__Bacillales;f__Staphylococcaceae;g__Staphylococcus;s__pasteuri-warneri	0.0%	0.0%	0.0%	0.0%	0.0%
	k__Bacteria;p__Proteobacteria;c__Alphaproteobacteria;o__Caulobacterales;f__Caulobacteraceae;g__Brevundimonas;s__nasdae-vesicularis	0.0%	0.0%	0.0%	0.1%	0.0%
	k__Bacteria;p__Proteobacteria;c__Alphaproteobacteria;o__Caulobacterales;f__Caulobacteraceae;g__Phenylobacterium;s__mobile	0.2%	0.1%	0.1%	0.4%	0.1%
	k__Bacteria;p__Proteobacteria;c__Alphaproteobacteria;o__Rhizobiales;f__Bradyrhizobiaceae;g__Afipia-Bradyrhizobium;s__NA	0.0%	0.0%	0.0%	0.1%	0.0%
	k__Bacteria;p__Proteobacteria;c__Alphaproteobacteria;o__Rhizobiales;f__Bradyrhizobiaceae;g__Bradyrhizobium;s__NA	0.1%	0.0%	0.6%	0.0%	0.0%
	k__Bacteria;p__Proteobacteria;c__Alphaproteobacteria;o__Rhizobiales;f__Bradyrhizobiaceae;g__NA;s__sp43311	0.4%	0.1%	0.0%	1.3%	0.1%
	k__Bacteria;p__Proteobacteria;c__Alphaproteobacteria;o__Rhizobiales;f__Hyphomicrobiaceae;g__Vasilyevaea;s__enhydra	0.0%	0.0%	0.0%	0.0%	0.0%
	k__Bacteria;p__Proteobacteria;c__Alphaproteobacteria;o__Rhizobiales;f__Methylocystaceae;g__Methylopila;s__jiangsuensis	0.0%	0.1%	0.0%	0.0%	0.0%
	k__Bacteria;p__Proteobacteria;c__Alphaproteobacteria;o__Rhizobiales;f__Phyllobacteriaceae;g__Mesorhizobium;s__amorphae	0.2%	0.0%	0.2%	0.5%	0.1%
	k__Bacteria;p__Proteobacteria;c__Alphaproteobacteria;o__Rhizobiales;f__Rhizobiaceae;g__Ensifer;s__sojae	0.1%	0.1%	0.1%	0.2%	0.0%
	k__Bacteria;p__Proteobacteria;c__Alphaproteobacteria;o__Rhodospirillales;f__NA;g__Reyranella;s__massiliensis	0.9%	0.2%	0.6%	2.8%	0.1%
	k__Bacteria;p__Proteobacteria;c__Alphaproteobacteria;o__Rickettsiales;f__NA;g__*Captivus;s__sp47053	0.0%	0.0%	0.0%	0.1%	0.0%
	k__Bacteria;p__Proteobacteria;c__Alphaproteobacteria;o__Sphingomonadales;f__Sphingomonadaceae;g__Novosphingobium;s__sp47622	0.0%	0.0%	0.0%	0.0%	0.0%
	k__Bacteria;p__Proteobacteria;c__Alphaproteobacteria;o__Sphingomonadales;f__Sphingomonadaceae;g__Sphingobium;s__herbicidovorans	0.0%	0.0%	0.0%	0.1%	0.0%
	k__Bacteria;p__Proteobacteria;c__Alphaproteobacteria;o__Sphingomonadales;f__Sphingomonadaceae;g__Sphingobium;s__yanoikuyae	0.4%	0.1%	0.5%	0.6%	0.2%
	k__Bacteria;p__Proteobacteria;c__Alphaproteobacteria;o__Sphingomonadales;f__Sphingomonadaceae;g__Sphingomonas;s__koreensis	0.9%	0.0%	0.2%	3.3%	0.0%
	k__Bacteria;p__Proteobacteria;c__Alphaproteobacteria;o__Sphingomonadales;f__Sphingomonadaceae;g__Sphingomonas;s__latericiarae	0.0%	0.0%	0.1%	0.0%	0.0%
	k__Bacteria;p__Proteobacteria;c__Alphaproteobacteria;o__Sphingomonadales;f__Sphingomonadaceae;g__Sphingomonas;s__sp47904	0.0%	0.0%	0.1%	0.1%	0.0%
	k__Bacteria;p__Proteobacteria;c__Alphaproteobacteria;o__Sphingomonadales;f__Sphingomonadaceae;g__Sphingopyxis;s__alaskensis-bauzanensis-chilensis	0.1%	0.0%	0.0%	0.3%	0.1%
	k__Bacteria;p__Proteobacteria;c__Betaproteobacteria;o__Burkholderiales;f__Alcaligenaceae;g__Achromobacter;s__pulmonis-xylosoxidans	0.0%	0.0%	0.0%	0.0%	0.0%
	k__Bacteria;p__Proteobacteria;c__Betaproteobacteria;o__Burkholderiales;f__Alcaligenaceae;g__Pigmentiphaga;s__litoralis	0.0%	0.0%	0.0%	0.1%	0.0%
	k__Bacteria;p__Proteobacteria;c__Betaproteobacteria;o__Burkholderiales;f__Comamonadaceae;g__Acidovorax;s__defluvii-radicis	0.3%	0.2%	0.3%	0.4%	0.1%
	k__Bacteria;p__Proteobacteria;c__Betaproteobacteria;o__Burkholderiales;f__Comamonadaceae;g__Acidovorax;s__delafieldii	0.0%	0.1%	0.0%	0.0%	0.0%
	k__Bacteria;p__Proteobacteria;c__Betaproteobacteria;o__Burkholderiales;f__Comamonadaceae;g__Acidovorax;s__temperans	0.0%	0.0%	0.1%	0.1%	0.0%
	k__Bacteria;p__Proteobacteria;c__Betaproteobacteria;o__Burkholderiales;f__Comamonadaceae;g__Delftia;s__acidovorans	0.0%	0.0%	0.1%	0.0%	0.0%
	k__Bacteria;p__Proteobacteria;c__Betaproteobacteria;o__Burkholderiales;f__Comamonadaceae;g__NA;s__sp49233	0.2%	0.0%	0.0%	0.9%	0.0%
	k__Bacteria;p__Proteobacteria;c__Betaproteobacteria;o__Burkholderiales;f__Comamonadaceae;g__Pelomonas;s__saccharophila	1.9%	1.2%	0.0%	5.8%	0.5%
	k__Bacteria;p__Proteobacteria;c__Betaproteobacteria;o__Burkholderiales;f__Comamonadaceae;g__Polaromonas;s__aquatica	0.0%	0.0%	0.0%	0.0%	0.0%
	k__Bacteria;p__Proteobacteria;c__Betaproteobacteria;o__Burkholderiales;f__Comamonadaceae;g__Pseudorhodoferax;s__sp49091	36.8%	50.7%	1.6%	6.3%	88.7%
	k__Bacteria;p__Proteobacteria;c__Betaproteobacteria;o__Burkholderiales;f__Comamonadaceae;g__Rhizobacter-Variovorax;s__bergeniae-sp49201	0.1%	0.0%	0.0%	0.2%	0.0%
	k__Bacteria;p__Proteobacteria;c__Betaproteobacteria;o__Burkholderiales;f__Comamonadaceae;g__Variovorax;s__boronicumulans	0.0%	0.0%	0.0%	0.0%	0.0%
	k__Bacteria;p__Proteobacteria;c__Betaproteobacteria;o__Burkholderiales;f__Comamonadaceae;g__Variovorax;s__ginsengisoli-paradoxus	0.0%	0.0%	0.0%	0.0%	0.0%
	k__Bacteria;p__Proteobacteria;c__Betaproteobacteria;o__Burkholderiales;f__Comamonadaceae;g__Variovorax;s__paradoxus	1.3%	0.0%	0.8%	4.5%	0.0%
	k__Bacteria;p__Proteobacteria;c__Betaproteobacteria;o__Burkholderiales;f__Comamonadaceae;g__Variovorax;s__sp49186	0.0%	0.0%	0.0%	0.0%	0.0%
	k__Bacteria;p__Proteobacteria;c__Betaproteobacteria;o__Burkholderiales;f__Oxalobacteraceae;g__Undibacterium;s__seohonense	0.2%	0.0%	0.6%	0.1%	0.2%
	k__Bacteria;p__Proteobacteria;c__Betaproteobacteria;o__Methylophilales;f__Methylophilaceae;g__Methylophilus;s__luteus-methylotrophus	0.1%	0.0%	0.0%	0.3%	0.0%
	k__Bacteria;p__Proteobacteria;c__Deltaproteobacteria;o__Myxococcales;f__Sandaracinaceae;g__NA;s__sp54084	0.0%	0.0%	0.1%	0.0%	0.0%
	k__Bacteria;p__Proteobacteria;c__Deltaproteobacteria;o__Oligoflexales;f__NA;g__NA;s__sp54466	0.0%	0.0%	0.0%	0.1%	0.0%
	k__Bacteria;p__Proteobacteria;c__Gammaproteobacteria;o__NA;f__NA;g__NA;s__sp61029	45.9%	44.9%	87.4%	45.3%	6.0%
	k__Bacteria;p__Proteobacteria;c__Gammaproteobacteria;o__Pseudomonadales;f__Moraxellaceae;g__Acinetobacter;s__bouvetii-johnsonii	0.0%	0.0%	0.0%	0.2%	0.0%
	k__Bacteria;p__Proteobacteria;c__Gammaproteobacteria;o__Pseudomonadales;f__Moraxellaceae;g__Acinetobacter;s__gyllenbergii-johnsonii-junii	0.1%	0.0%	0.0%	0.3%	0.0%
	k__Bacteria;p__Proteobacteria;c__Gammaproteobacteria;o__Pseudomonadales;f__Moraxellaceae;g__Acinetobacter;s__haemolyticus-johnsonii-lwoffii	0.0%	0.0%	0.0%	0.1%	0.0%
	k__Bacteria;p__Proteobacteria;c__Gammaproteobacteria;o__Pseudomonadales;f__Moraxellaceae;g__Acinetobacter;s__johnsonii	0.0%	0.0%	0.1%	0.0%	0.0%
	k__Bacteria;p__Proteobacteria;c__Gammaproteobacteria;o__Pseudomonadales;f__Moraxellaceae;g__Acinetobacter;s__johnsonii-lwoffii	0.0%	0.0%	0.1%	0.0%	0.0%
	k__Bacteria;p__Proteobacteria;c__Gammaproteobacteria;o__Pseudomonadales;f__Moraxellaceae;g__Perlucidibaca;s__sp62642-sp62643	0.0%	0.0%	0.0%	0.0%	0.0%
	k__Bacteria;p__Proteobacteria;c__Gammaproteobacteria;o__Pseudomonadales;f__Pseudomonadaceae;g__Pseudomonas;s__NA	0.1%	0.0%	0.1%	0.1%	0.0%
	k__Bacteria;p__Proteobacteria;c__Gammaproteobacteria;o__Pseudomonadales;f__Pseudomonadaceae;g__Pseudomonas;s__arsenicoxydans-mandelii-marginalis	0.1%	0.0%	0.0%	0.2%	0.0%
	k__Bacteria;p__Proteobacteria;c__Gammaproteobacteria;o__Pseudomonadales;f__Pseudomonadaceae;g__Pseudomonas;s__azotoformans-fluorescens-synxantha	0.0%	0.0%	0.0%	0.1%	0.0%
	k__Bacteria;p__Proteobacteria;c__Gammaproteobacteria;o__Pseudomonadales;f__Pseudomonadaceae;g__Pseudomonas;s__brenneri-fluorescens-proteolytica	0.2%	0.0%	0.0%	0.9%	0.0%
	k__Bacteria;p__Proteobacteria;c__Gammaproteobacteria;o__Pseudomonadales;f__Pseudomonadaceae;g__Pseudomonas;s__costantinii-fluorescens-poae	0.1%	0.0%	0.1%	0.2%	0.0%
	k__Bacteria;p__Proteobacteria;c__Gammaproteobacteria;o__Pseudomonadales;f__Pseudomonadaceae;g__Pseudomonas;s__fluorescens-gessardii-libanensis	0.0%	0.0%	0.1%	0.0%	0.0%
	k__Bacteria;p__Proteobacteria;c__Gammaproteobacteria;o__Pseudomonadales;f__Pseudomonadaceae;g__Pseudomonas;s__hunanensis-plecoglossicida-putida	0.2%	0.0%	0.0%	0.7%	0.1%
	k__Bacteria;p__Proteobacteria;c__Gammaproteobacteria;o__Pseudomonadales;f__Pseudomonadaceae;g__Pseudomonas;s__stutzeri	0.0%	0.0%	0.0%	0.0%	0.0%
	k__Bacteria;p__Proteobacteria;c__Gammaproteobacteria;o__Xanthomonadales;f__Xanthomonadaceae;g__Stenotrophomonas;s__maltophilia	0.0%	0.0%	0.0%	0.1%	0.0%

Table 2. Microbial composition of *Girardia tigrina* microbiota at species level.

Well Number	Carbon Source	Compound Group
A1	Water	--
B1	Pyruvic acid methyl ester	Carbohydrates
C1	Tween 40	Polymers
D1	Tween 80	Polymers
E1	α-Cyclodextrin	Polymers
F1	Glycogen	Polymers
G1	D-Cellobiose	Carbohydrates
H1	α-D-Lactose	Carbohydrates
A2	β-Methyl-D-glucoside	Carbohydrates
B2	D-Xylose	Carbohydrates
C2	i-Erythritol	Carbohydrates
D2	D-Mannitol	Carbohydrates
E2	N-Acetyl-D-glucosamine	Carbohydrates
F2	D-Glucosaminic acid	Carboxylic and ketonic acids
G2	Glucose-1-phosphate	Carbohydrates
H2	D,L-α-Glycerol phosphate	Carbohydrates
A3	D-Galactonic acid-γ-lactone	Carboxylic and ketonic acids
B3	D-Galacturonic acid	Carboxylic and ketonic acids
C3	2-Hydroxybenzoic acid	Carboxylic and ketonic acids
D3	4-Hydroxybenzoic acid	Carboxylic and ketonic acids
E3	γ-Hydroxybutyric acid	Carboxylic and ketonic acids
F3	Itaconic acid	Carboxylic and ketonic acids
G3	α-Ketobutyric acid	Carboxylic and ketonic acids
H3	D-Malic acid	Carboxylic and ketonic acids
A4	L-Arginine	Amino Acids
B4	L-Asparagine	Amino Acids
C4	L-Phenylalanine	Amino Acids
D4	L-Serine	Amino Acids
E4	L-Threonine	Amino Acids
F4	Glycyl-L-glutamic acid	Amino Acids
G4	Phenylethylamine	Amines/amides
H4	Putrescine	Amines/amides

Table 3. Biolog EcoPlate™ carbon source guild groupings (Gryta *et al.*, 2014)

	ZnO + Planaria		CuSi + Planaria		TBCC + Planaria	
	Live	Dead	Live	Dead	Live	Dead
0.1 mg/ml	3	0	3	0	3	0
1.0 mg/ml	1	2	0	3	3	0
2.0 mg/ml	1	2	2	1	3	0
5.0 mg/ml	0	3	0	3	3	0
10 mg/ml	0	3	1	2	3	0
20 mg/ml	3	0	0	3	3	0

Table 4. Mortality of planarian *Girardia tigrina* when exposed to various concentrations and types of MCNPs. Ideal concentrations of MCNPs used to expose planarian microbiome were pulled from toxicity data.

References

Applerot, G., Lellouche, J., Lipovsky, A., Nitzan, Y., Lubart, R., Gedanken, A., & Banin, E. (2012). Understanding the antibacterial mechanism of CuO nanoparticles: revealing the route of induced oxidative stress. *Small (Weinheim an der Bergstrasse, Germany), 8*(21), 3326–3337. https://doi.org/10.1002/smll.201200772

Arnold, C. P., Merryman, M. S., Harris-Arnold, A., Mckinney, S. A., Seidel, C. W., Loethen, S., Proctor, K. N., Guo, L., & Sánchez Alvarado, A. (2016). Pathogenic shifts in endogenous microbiota impede tissue regeneration via distinct activation of TAK1/MKK/p38. *Elife*, *5*. https://doi.org/10.7554/elife.16793

Bahadar H, Maqbool F, Niaz K, Abdollahi M. Toxicity of Nanoparticles and an Overview of Current Experimental Models. Iran Biomed J. 2016;20(1):1-11. doi: 10.7508/ibj.2016.01.001. Epub 2015 Aug 19.

Bertoglio, F., Bloise, N., Oriano, M., Petrini, P., Sprio, S., Imbriani, M., Visai, L. (2018). Treatment of Biofilm Communities: An Update on New Tools from the Nanosized World. *Applied Sciences, 8*(6), 845. https://doi.org/10.3390/app8060845

Bhatia, S. (2016). *Nanoparticles Types, Classification, Characterization, Fabrication Methods and Drug Delivery Applications*. *Natural Polymer Drug Delivery Systems*, 33-93. https://doi.org/doi:10.1007/978-3-319-41129-3_2

Bijnens, K., Thijs, S., Leynen, N., Stevens, V., McAmmond, B., Van Hamme, J., Smeets, K. (2021). Differential effect of silver nanoparticles on the microbiome of adult anddeveloping planaria. In. Aquatic Toxicology: Elsevier.

Bjarnsholt, T. (2013). The role of bacterial biofilms in chronic infections. *APMIS, 121*, 1-58. https://doi.org/10.1111/apm.12099

Blaak, E. E., Canfora, E. E., Theis, S., Frost, G., Groen, A. K., Mithieux, G., Verbeke, K. (2020). Short chain fatty acids in human gut and metabolic health. *Beneficial Microbes, 11*(5), 411-455. https://doi.org/10.3920/bm2020.0057

Bochner, B. R. (1989). Sleuthing out bacterial identities. *Nature, 339*(6220), 157-158. https://doi.org/10.1038/339157a0

Brown, M. R. W., Allison, D. G., & Gilbert, P. (1988). Resistance of bacterial biofilms to antibiotics a growth-rate related effect? *Journal of Antimicrobial Chemotherapy*, *22*(6), 777-780. https://doi.org/10.1093/jac/22.6.777

Bäckhed, F., Roswall, J., Peng, Y., Feng, Q., Jia, H., Kovatcheva-Datchary, P., Wang, J. (2015). Dynamics and Stabilization of the Human Gut Microbiome during the First Year of Life. *Cell Host & Microbe, 17*(5), 690-703. https://doi.org/https://doi.org/10.1016/j.chom.2015.04.004

Chu, H., Khosravi, A., Kusumawardhani, I. P., Kwon, A. H. K., Vasconcelos, A. C., Cunha, L. D., Mazmanian, S. K. (2016). Gene-microbiota interactions contribute to the

pathogenesis of inflammatory bowel disease. *Science*, *352*(6289), 1116-1120. https://doi.org/10.1126/science.aad9948

Corrêa-Oliveira, R., Fachi, J. L., Vieira, A., Sato, F. T., & Vinolo, M. A. R. (2016). Regulation of immune cell function by short-chain fatty acids. *Clinical & Translational Immunology*, *5*(4), e73. https://doi.org/10.1038/cti.2016.17

Costerton, J., Stewart, P., & Greenberg, E. (1999). Bacterial biofilms: a common cause of persistent infections. *Science*, *284*(5418), 1318-1322. https://doi.org/10.1126/science.284.5418.1318.

Costerton, J. W., Montanaro, L., & Arciola, C. R. (2005). Biofilm in implant infections: its production and regulation. *The International journal of artificial organs*, *28*(11), 1062-1068. https://doi.org/https://doi.org/10.1177/039139880502801103

Dadi, R., Azouani, R., Traore, M., Mielcarek, C., & Kanaev, A. (2019). Antibacterial activity of ZnO and CuO nanoparticles against gram positive and gram-negative strains. *Materials science & engineering. C, Materials for biological applications*, *104*, 109968. https://doi.org/10.1016/j.msec.2019.109968

De La Fuente-Núñez, C., Reffuveille, F., Fernández, L., & Hancock, R. E. (2013). Bacterial biofilm development as a multicellular adaptation: antibiotic resistance and new therapeutic strategies. *Current Opinion in Microbiology*, *16*(5), 580-589. https://doi.org/10.1016/j.mib.2013.06.013

Deres, P., Halmosi, R., Toth, A., Kovacs, K., Palfi, A., Habon, T., Toth, K. (2005). Prevention of doxorubicin-induced acute cardiotoxicity by an experimental antioxidant compound. *Journal of Cardiovascular Pharmacology*, *45*(1), 36-43. https://doi.org/10.1097/00005344-200501000-00007

Desireddy, A., Conn, B. E., Guo, J., Yoon, B., Barnett, R. N., Monahan, B. M., Bigioni, T. P. (2013). Ultrastable silver nanoparticles. *Nature*, *501*(7467), 399-402. https://doi.org/10.1038/nature12523

Ding, J., Liu, J., Chang, X. B., Zhu, D., & Lassen, S. B. (2020). Exposure of CuO nanoparticles and their metal counterpart leads to change in the gut microbiota and resistome of collembolans. *Chemosphere*, *258*, 127347. https://doi.org/10.1016/j.chemosphere.2020.127347

Ding, X., Song, L., Han, Y., Wang, Y., Tang, X., Cui, G., & Xu, Z. (2019). Effects of Fe^{3+} on Acute Toxicity and Regeneration of Planarian (*Dugesia japonica*) at Different Temperatures. *BioMed research international*, *2019*, 8591631. https://doi.org/10.1155/2019/8591631

Docter, D., Westmeier, D., Markiewicz, M., Stolte, S., Knauer, S. K., & Stauber, R. H. (2015). The nanoparticle biomolecule corona: lessons learned – challenge accepted? *Chemical Society Reviews*, *44*(17), 6094-6121. https://doi.org/10.1039/c5cs00217f

Dunne, W. M., Mason, E. O., & Kaplan, S. L. (1993). Diffusion of rifampin and vancomycin through a Staphylococcus epidermidis biofilm. *Antimicrobial Agents and Chemotherapy*, *37*(12), 2522-2526. https://doi.org/10.1128/aac.37.12.2522

Feng, Y., Min, L., Zhang, W., Liu, J., Hou, Z., Chu, M., Zhang, H. (2017). Zinc Oxide Nanoparticles Influence Microflora in Ileal Digesta and Correlate Well with Blood Metabolites. *Frontiers in microbiology*, *8*, 992. https://doi.org/https://doi.org/10.3389/fmicb.2017.00992

Flemming, H.-C. (2016). EPS—Then and Now. *Microorganisms*, *4*(4), 41. https://doi.org/10.3390/microorganisms4040041

Flemming, H.-C., Wingender, J., Szewzyk, U., Steinberg, P., Rice, S. A., & Kjelleberg, S. (2016). Biofilms: an emergent form of bacterial life. *Nature Reviews Microbiology*, *14*(9), 563-575. https://doi.org/10.1038/nrmicro.2016.94

Fulaz, S., Vitale, S., Quinn, L., & Casey, E. (2019). Nanoparticle–Biofilm Interactions: The Role of the EPS Matrix. *Trends in Microbiology*, *27*(11), 915-926. https://doi.org/10.1016/j.tim.2019.07.004

Ghebretatios, M., Schaly, S., & Prakash, S. (2021). Nanoparticles in the Food Industry and Their Impact on Human Gut Microbiome and Diseases. *International Journal of Molecular Sciences*, *22*(4), 1942. https://doi.org/10.3390/ijms22041942

Grissa, I., Elghoul, J., Ezzi, L., Chakroun, S., Kerkeni, E., Hassine, M., Haouas, Z. (2015). Anemia and genotoxicity induced by sub-chronic intragastric treatment of rats with titanium dioxide nanoparticles. *Mutation Research/Genetic Toxicology and Environmental Mutagenesis*, *794*, 25-31. https://doi.org/10.1016/j.mrgentox.2015.09.005

Gryta, A., Frąc, M., & Oszust, K. (2014). The Application of the Biolog EcoPlate™ Approach in Ecotoxicological Evaluation of Dairy Sewage Sludge. *Applied Biochemistry and Biotechnology*, *174*(4), 1434-1443. https://doi.org/10.1007/s12010-014-1131-8

Hagstrom, D., Hirokawa, H., Zhang, L., Radic, Z., Taylor, P., & Collins, E. S. (2017). Planarian cholinesterase: in vitro characterization of an evolutionarily ancient enzyme to study organophosphorus pesticide toxicity and reactivation. *Archives of toxicology*, *91*(8), 2837–2847. https://doi.org/10.1007/s00204-016-1908-3

Hall-Stoodley, L., Costerton, J. W., & Stoodley, P. (2004). Bacterial biofilms: from the Natural environment to infectious diseases. *Nature Reviews Microbiology*, *2*(2), 95-108. https://doi.org/10.1038/nrmicro821

Han, Y., Zhang, X., Liu, P., Xu, S., Chen, D., Liu, J. N., & Xie, W. (2022). Microplastics exposure causes oxidative stress and microbiota dysbiosis in planarian Dugesia japonica. *Environmental Science and Pollution Research*, *29*(19), 28973–28983. https://doi.org/10.1007/s11356-022-18547-x

Harrison, F. (2007). Microbial ecology of the cystic fibrosis lung. *Microbiology*, *153*(4), 917–923. https://doi.org/10.1099/mic.0.2006/004077-0

Hevia, A., Delgado, S., Sánchez, B., & Margolles, A. (2015). Molecular Players Involved in the Interaction Between Beneficial Bacteria and the Immune System. In (Vol. 6, pp. 1285): *Frontiers in microbiology*.

Høiby, N., Ciofu, O., Johansen, H. K., Song, Z. J., Moser, C., Jensen, P. Ø., Bjarnsholt, T. (2011). The clinical impact of bacterial biofilms. *International Journal of Oral Science*, *3*(2), 55-65. https://doi.org/10.4248/ijos11026

Ikuma, K., Decho, A. W., & Lau, B. L. T. (2015). When nanoparticles meet biofilms-interactions guiding the environmental fate and accumulation of nanoparticles. *Frontiers in Microbiology*., *6*, 591. https://doi.org/10.3389/fmicb.2015.00591

Innocenzi, P., & Stagi, L. (2020). Carbon-based antiviral nanomaterials: graphene, C-dots, and fullerenes. A perspective. *Chemical Science*, *11*(26), 6606-6622. https://doi.org/10.1039/d0sc02658a

Ivankovic, M., Haneckova, R., Thommen, A., Grohme, M. A., Vila-Farré, M., Werner, S., & Rink, J. C. (2019). Model systems for regeneration: planarians. *Development (Cambridge, England)*, *146*(17), dev167684. https://doi.org/10.1242/dev.167684

James, G. A., Beaudette, L., & Costerton, J. W. (1995). Interspecies bacterial interactions in biofilms. *Journal of Industrial Microbiology*, *15*(4), 257–262. https://doi.org/10.1007/bf01569978

Javurek, A. B., Suresh, D., Spollen, W. G., Hart, M. L., Hansen, S. A., Ellersieck, M. R., Rosenfeld, C. S. (2017). Gut Dysbiosis and Neurobehavioral Alterations in Rats Exposed to Silver Nanoparticles. *Scientific Reports*, *7*(1). https://doi.org/10.1038/s41598-017-02880-0

Kaur, T., Putatunda, C., Vyas, A., & Kumar, G. (2021). Zinc oxide nanoparticles inhibit bacterial biofilm formation via altering cell membrane permeability. *Preparative biochemistry & biotechnology*, *51*(4), 309–319. https://doi.org/10.1080/10826068.2020.1815057

Ke, P. C., Lin, S., Parak, W. J., Davis, T. P., & Caruso, F. (2017). A Decade of the Protein Corona. *ACS nano*, *11*(12), 11773-11776. https://doi.org/10.1021/acsnano.7b08008

Khatoon, Z., McTiernan, C. D., Suuronen, E. J., Mah, T. F., & Alarcon, E. I. (2018). Bacterial biofilm formation on implantable devices and approaches to its treatment and prevention. *Heliyon*, *4*(12). https://doi.org/https://doi.org/10.1016/j.heliyon.2018.e01067

Lee, K. W. K., Periasamy, S., Mukherjee, M., Xie, C., Kjelleberg, S., & Rice, S. A. (2014). Biofilm development and enhanced stress resistance of a model, mixed-species community biofilm. *The ISME Journal*, *8*(4), 894-907. https://doi.org/10.1038/ismej.2013.194

Leblanc, J. G., Milani, C., De Giori, G. S., Sesma, F., Van Sinderen, D., & Ventura, M. (2013). Bacteria as vitamin suppliers to their host: a gut microbiota perspective. *Current Opinion in Biotechnology*, *24*(2), 160-168. https://doi.org/10.1016/j.copbio.2012.08.005

Lewis, K. (2007). Persister cells, dormancy and infectious disease. *Nature Reviews Microbiology*, *5*(1), 48-56. https://doi.org/10.1038/nrmicro1557

Leynen, N., Van Bellegem, F., Wouters, A., Bove, H., Ploem, J.-P., Thijssen, E., Smeets, K. (2019). *In vivo Toxicity Assessment of Silver Nanoparticles in Homeostaticversus Regenerating Planarians*. https://doi.org/10.1080/17435390.2018.1553252

Li, J., Tang, M., & Xue, Y. (2018). Review of the effects of sliver nanoparticle exposure on gutbacteria. In. Journal of Applied Toxicology: Wiley.

Li, W.-R., Xie, X.-B., Shi, Q.-S., Zeng, H.-Y., Ou-Yang, Y.-S., & Chen, Y.-B. (2010). Antibacterial activity and mechanism of silver nanoparticles on Escherichia coli. *Applied Microbiology and Biotechnology*, *85*(4), 1115–1122. https://doi.org/10.1007/s00253-009-2159-5

Liu, X., Xu, Y., Wu, Z., & Chen, H. (2013). Poly(N-vinylpyrrolidone)-Modified Surfaces for Biomedical Applications. *Macromolecular Bioscience*, *13*, 147 - 154.

Louis, P., & Flint, H. J. (2017). Formation of propionate and butyrate by the human colonic microbiota. *Environmental Microbiology*, *19*(1), 29-41. https://doi.org/10.1111/1462-2920.13589

Louis, P., Hold, G. L., & Flint, H. J. (2014). The gut microbiota, bacterial metabolites, and colorectal cancer. *Nature Reviews Microbiology*, *12*(10), 661-672. https://doi.org/10.1038/nrmicro3344

Mazmanian, S. K., Liu, C. H., Tzianabos, A. O., & Kasper, D. L. (2005). An Immunomodulatory Molecule of Symbiotic Bacteria Directs Maturation of the Host Immune System. *Cell*, *122*(1), 107-118. https://doi.org/10.1016/j.cell.2005.05.007

Miles, R. D., O'Keefe, S. F., Henry, P. R., Ammerman, C. B., & Luo, X. G. (1998). The effect of dietary supplementation with copper sulfate or tribasic copper chloride on broiler performance, relative copper bioavailability, and dietary prooxidant activity. *Poultry science*, *77*(3), 416–425. https://doi.org/10.1093/ps/77.3.416

Miller, K. P., Wang, L., Benicewiczb, B. C., & Decho, A. W. (2015). Inorganic nanoparticles engineered to attack bacteria. *Chem Soc Rev.*, *44*(21), 7787-7807. https://doi.org/10.1039/c5cs00041f

Moons, P., Michiels, C.W. and Aertsen, A. (2009) Bacterial Interactions in Biofilms. Criticals Reviews in Microbiology, 35, 157-168. http://dx.doi.org/10.1080/10408410902809431

Morones, J. R., Elechiguerra, J. L., Camacho, A., Holt, K., Kouri, J. B., Ramirez, J. T., & Yacaman, M. J. (2005). The bactericidal effect of silver nanoparticles. *Nanotechnology*, *16*, 2346-2353. https://doi.org/http://dx.doi.org/10.1088/0957-4484/16/10/059

Morrison, D. J., & Preston, T. (2016). Formation of short chain fatty acids by the gut microbiota and their impact on human metabolism. *Gut Microbes*, *7*(3), 189-200. https://doi.org/10.1080/19490976.2015.1134082

Mu, Q., Jiang, G., Chen, L., Zhou, H., Fourches, D., Tropsha, A., & Yan, B. (2014). Chemical Basis of Interactions Between Engineered Nanoparticles and Biological Systems. *Chemical Reviews*, *114*(15), 7740-7781. https://doi.org/10.1021/cr400295a

Musial, J., Krakowiak, R., Mlynarczyk, D. T., Goslinski, T., & Stanisz, B. J. (2020). Titanium Dioxide Nanoparticles in Food and Personal Care Products—What Do We Know about Their Safety? *Nanomaterials*, *10*(6), 1110. https://doi.org/10.3390/nano10061110

Nadell, C. D., Drescher, K., Wingreen, N. S., & Bassler, B. L. (2015). Extracellular matrix structure governs invasion resistance in bacterial biofilms. *The ISME Journal*, *9*(8), 1700-1709. https://doi.org/10.1038/ismej.2014.246

Navarro-Mabarak, C., Camacho-Carranza, R., & Espinosa-Aguirre, J. (2018). Cytochrome P450 in the central nervous system as a therapeutic target in neurodegenerative diseases. *Drug Metab Rev*, *50*(2), 95-108. https://doi.org/10.1080/03602532.2018.1439502

Németh, I., Molnár, S., Vaszita, E., & Molnár, M. (2021). The Biolog EcoPlate™ Technique for Assessing the Effect of Metal Oxide Nanoparticles on Freshwater Microbial Communities. *Nanomaterials*, *11*(7), 1777. https://doi.org/10.3390/nano11071777

Pagán, O. R. (2017). Planaria: an animal model that integrates development, regeneration, and pharmacology. *The International Journal of Developmental Biology*, *61*(8-9), 519-529. https://doi.org/10.1387/ijdb.160328op

Pagán, O. R., Baker, D., Deats, S., Montgomery, E., Tenaglia, M., Randolph, C., Raffa, R. B. (2012). Planarians in pharmacology: parthenolide is a specific behavioral antagonist of cocaine in the planarian Girardia tigrina. *The International Journal of Developmental Biology*, *56*(1-2-3), 193-196. https://doi.org/10.1387/ijdb.113486op

Pascale, A., Marchesi, N., Marelli, C., Coppola, A., Luzi, L., Govoni, S., Gazzaruso, C. (2018). *Microbiota and metabolic diseases* https://doi.org/https://doi.org/10.1007/s12020-018-1605-5

Pei, X., Xiao, Z., Liu, L., Wang, G., Tao, W., Wang, M., Leng, D. (2018). Effects of dietary zinc oxide nanoparticles supplementation on growth performance, zinc status, intestinal morphology, microflora population, and immune response in weaned pigs. *Journal of the Science of Food and Agriculture*, *99*(3), 1366-1374. https://doi.org/10.1002/jsfa.9312

Petersson, J., Schreiber, O., Hansson, G. C., Gendler, S. J., Velcich, A., Lundberg, J. O., . . . Phillipson, M. (2011). Importance and regulation of the colonic mucus barrier in a mouse model of colitis. In (pp. 300(302), G327 - G333): *American journal of physiology, Gastrointestinal and liver physiology*.

Petosa, A. R., Jaisi, D. P., Quevedo, I. R., Elimelech, M., & Tufenkji, N. (2010). Aggregation and Deposition of Engineered Nanomaterials in Aquatic Environments: Role of Physicochemical Interactions. *Environmental Science & Technology*, *44*(17), 6532-6549. https://doi.org/10.1021/es100598h

Poole, K. (2001). Multidrug resistance in Gram-negative bacteria. *Current Opinion in Microbiology*, *4*(5), 500-508. https://doi.org/10.1016/s1369-5274(00)00242-3

Pourmortazavi, S. M., Marashianpour, Z., Karimi, M. S., & Mohammad-Zadeh, M. (2015). Electrochemical synthesis and characterization of zinc carbonate and zinc oxide nanoparticles. *Journal of Molecular Structure*, *1099*, 232-238. https://doi.org/10.1016/j.molstruc.2015.06.044

Raghunath, A., & Perumal, E. (2017). Metal oxide nanoparticles as antimicrobial agents: a promise for the future. *Int J Antimicrob Agents*, *49*(2), 137-152. https://doi.org/10.1016/j.ijantimicag.2016.11.011

Rimondini, L., Cochis, A., Varoni, E., Azzimonti, B., Carrassi, A., & Antoniac, I. V. (2014). *Biofilm Formation on Implants and Prosthetic Dental Materials*. Springer International Publishing. https://doi.org/https://doi.org/10.1007/978-3-319-09230-0_48-1

Römling, U., & Balsalobre, C. (2012). Biofilm infections, their resilience to therapy and innovative treatment strategies. *Journal of Internal Medicine*, *272*(6), 541-561. https://doi.org/10.1111/joim.12004

Rosa, M. T., & Loreto, E. L. S. (2019). The Catenulida flatworm can express genes from its microbiome or from the DNA it ingests. *Scientific Reports*, *9*(1). https://doi.org/10.1038/s41598-019-55659-w

Salesa, B., Martí, M., Frígols, B., & Serrano-Aroca, Á. (2019). Carbon Nanofibers in Pure Form and in Calcium Alginate Composites Films: New Cost-Effective Antibacterial Biomaterials against the Life-Threatening Multidrug-Resistant Staphylococcus epidermidis. *Polymers*, *11*(3), 453. https://doi.org/10.3390/polym11030453

Sánchez-López, E., Gomes, D., Esteruelas, G., Bonilla, L., Lopez-Machado, A. L., Galindo, R., Cano, A., Espina, M., Ettcheto, M., Camins, A., Silva, A. M., Durazzo, A., Santini, A., Garcia, M. L., & Souto, E. B. (2020). Metal-Based Nanoparticles as Antimicrobial Agents: An Overview. *Nanomaterials*, *10*(2), 292. https://doi.org/10.3390/nano10020292

Syafiuddin, A., Salmiati, S., Hadibarata, T., Kueh, A. B. H., Salim, M. R., & Zaini, M. A. A. (2018). Silver Nanoparticles in the Water Environment in Malaysia: Inspection, characterization, removal, modeling, and future perspective. *Scientific Reports*, *8*(1). https://doi.org/10.1038/s41598-018-19375-1

Sender, R., Fuchs, S., & Milo, R. (2016). Revised Estimates for the Number of Human and Bacteria Cells in the Body. *PLOS Biology*, *14*(8), e1002533. https://doi.org/10.1371/journal.pbio.1002533

Serrano-Aroca, Á., Takayama, K., Tuñón-Molina, A., Seyran, M., Hassan, S. S., Pal Choudhury, P., Brufsky, A. (2021). Carbon-Based Nanomaterials: Promising Antiviral Agents to Combat COVID-19 in the Microbial-Resistant Era. *ACS Nano*, *15*(5), 8069-8086. https://doi.org/10.1021/acsnano.1c00629

Studer, A. M., Limbach, L. K., Van Duc, L., Krumeich, F., Athanassiou, E. K., Gerber, L. C., Moch, H., & Stark, W. J. (2010). Nanoparticle cytotoxicity depends on intracellular solubility: comparison of stabilized copper metal and degradable copper oxide nanoparticles. *Toxicology letters*, *197*(3), 169–174. https://doi.org/10.1016/j.toxlet.2010.05.012

Swanson, P. A., Kumar, A., Samarin, S., Vijay-Kumar, M., Kundu, K., Murthy, N., Neish, A. S. (2011). Enteric commensal bacteria potentiate epithelial restitution via reactive oxygen species-mediated inactivation of focal adhesion kinase phosphatases. *Proceedings of the National Academy of Sciences*, *108*(21), 8803-8808. https://doi.org/10.1073/pnas.1010042108

Thursby, E., & Juge, N. (2017). Introduction to the human gut microbiota. *Biochemical Journal*, *474*(11), 1823-1836. https://doi.org/10.1042/bcj20160510

Tolson, A. H., & Wang, H. (2010). Regulation of drug-metabolizing enzymes by xenobiotic receptors: PXR and CAR. *Advanced Drug Delivery Reviews*, *62*(13), 1238-1249. https://doi.org/10.1016/j.addr.2010.08.006

Urrutia-Ortega, I. M., Garduño-Balderas, L. G., Delgado-Buenrostro, N. L., Freyre-Fonseca, V., Flores-Flores, J. O., González-Robles, A., Chirino, Y. I. (2016). Food-grade titanium dioxide exposure exacerbates tumor formation in colitis associated cancer model. *Food and Chemical Toxicology*, *93*, 20-31. https://doi.org/10.1016/j.fct.2016.04.014

Wang, X., Liu, X., Chen, J., Han, H., & Yuan, Z. (2014). Evaluation and mechanism of antifungal effects of carbon nanomaterials in controlling plant fungal pathogen. *Carbon*, *68*, 798-806. https://doi.org/https://doi.org/10.1016/j.carbon.2013.11.072.

Wang, Y., Tang, H., Xu, M., Luo, J., Zhao, L., Shi, F., Li, Y. (2019). Effect of copper nanoparticles on brain cytochrome P450 enzymes in rats. *Molecular Medicine Reports*. https://doi.org/10.3892/mmr.2019.10302

Williams, K., Milner, J., Boudreau, M., Gokulan, K., Cerniglia, C., & Khare, S. (2014). Effects of subchronic exposure of silver nanoparticles on intestinal microbiota and gut-associated immune responses in the ileum ofSprague-Dawley rats. In. Nanotoxicology: Informa healthcare.

Wu, J. P., & Li, M. H. (2018). The use of freshwater planarians in environmental toxicology studies: Advantages and potential. *Ecotoxicology and environmental safety*, *161*, 45–56. https://doi.org/10.1016/j.ecoenv.2018.05.057

Xia, T., Lai, W., Han, M., Han, M., Ma, X., & Zhang, L. (2017). Dietary ZnO nanoparticles alters intestinal microbiota and inflammation response in weaned piglets. *Oncotarget*, *8*(39), 64878-64891. https://doi.org/10.18632/oncotarget.17612

Yin, W., Wang, Y., Liu, L., & He, J. (2019). Biofilms: The Microbial "Protective Clothing" in Extreme Environments. *International Journal of Molecular Sciences*, *20*(14), 3423. https://doi.org/10.3390/ijms20143423

Yu, W., Liao, J., Yang, F., Zhang, H., Chang, X., Yang, Y., Bilal, R. M., Wei, G., Liang, W., Guo, J., & Tang, Z. (2021). Chronic tribasic copper chloride exposure induces rat liver damage by disrupting the mitophagy and apoptosis pathways. *Ecotoxicology and environmental safety*, *212*, 111968. https://doi.org/10.1016/j.ecoenv.2021.111968

Zhang, L., & Mah, T.-F. (2008). Involvement of a Novel Efflux System in Biofilm-Specific Resistance to Antibiotics. *Journal of Bacteriology*, *190*(13), 4447-4452. https://doi.org/10.1128/jb.01655-07

Zhang, X., Li, W., & Yang, Z. (2015). Toxicology of nanosized titanium dioxide: an update. *Archives of Toxicology*, *89*(12), 2207-2217. https://doi.org/10.1007/s00204-015-1594-6

Zheng, P., Pu, B., Yu, B., He, J., Yu, J., Mao, X., Chen, D. (2017). The differences between copper sulfate and tribasic copper chloride on growth performance, redox status,

deposition in tissues of pigs, and excretion in feces. *Asian-Australasian Journal of Animal Sciences, 31*(6), 873-880. https://doi.org/10.5713/ajas.17.0516

Łoczechin, A., Séron, K., Barras, A., Giovanelli, E., Belouzard, S., Chen, Y.-T., Szunerits, S. (2019). Functional Carbon Quantum Dots as Medical Countermeasures to Human Coronavirus. *ACS Applied Materials & Interfaces*, *11*(46), 42964-42974. https://doi.org/10.1021/acsami.9b15032